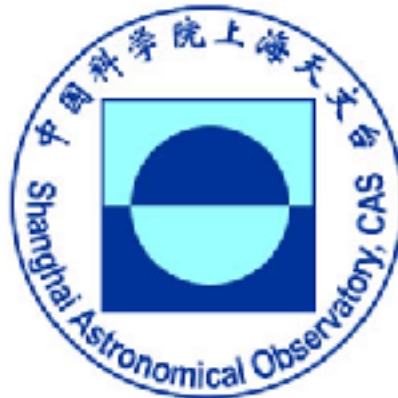


The Circumgalactic Medium and Fermi Bubbles in the Milky Way

Fulai Guo (郭福来)

Shanghai Astronomical Observatory

Chinese Academy of Sciences



Tsinghua Astro Colloquium, June 4, 2020

Relevant New Papers

Guo, Fulai*; Zhang, Ruiyu; Fang, Xiang-Er, 2020, under review w/ Nature Astronomy

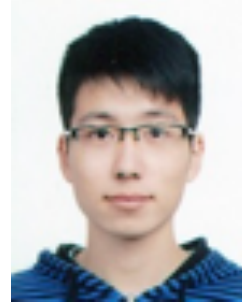
Fang, Xiang-Er; **Guo, Fulai***; Yuan, Ye-Fei, 2020, ApJ

Zhang, Ruiyu; **Guo, Fulai***, 2020, ApJ

Collaborators



Ruiyu Zhang



Shaokun Xie



Yuezhen Ye



Xiang'er Fang



Ye-Fei Yuan
(UCTC)



Wei Miao



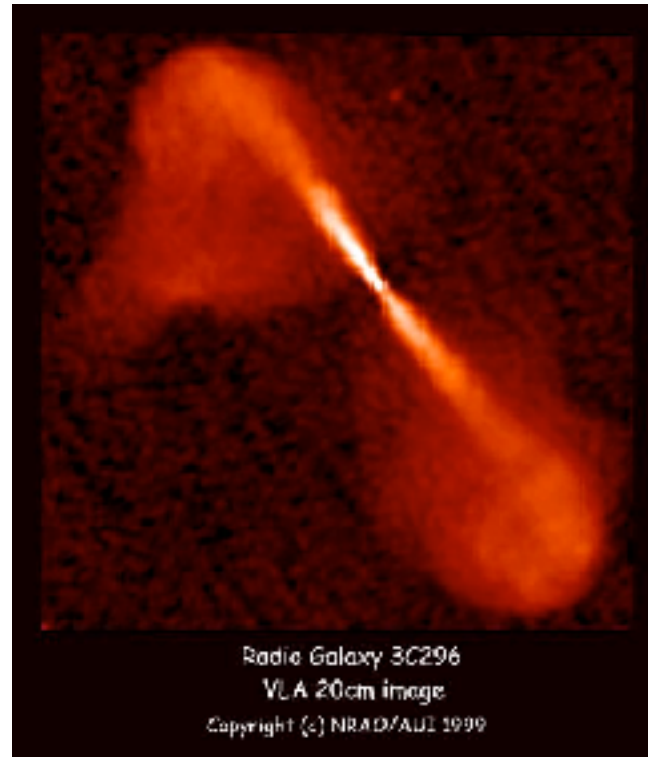
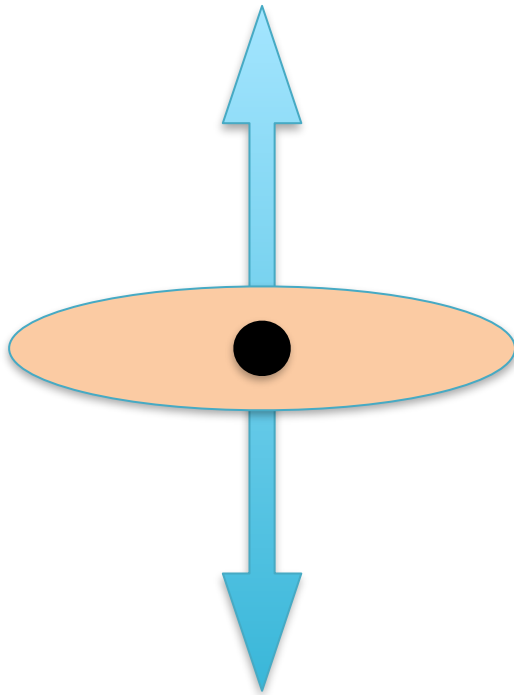
Xiaodong Duan

Talk Outline

- A physically-motivated model for CGM in the Milky Way
- Weighing the Milky Way with its CGM
- Cooling Flows in the Milky Way
- The new forward shock model of the Fermi Bubbles

How did the MW story start?

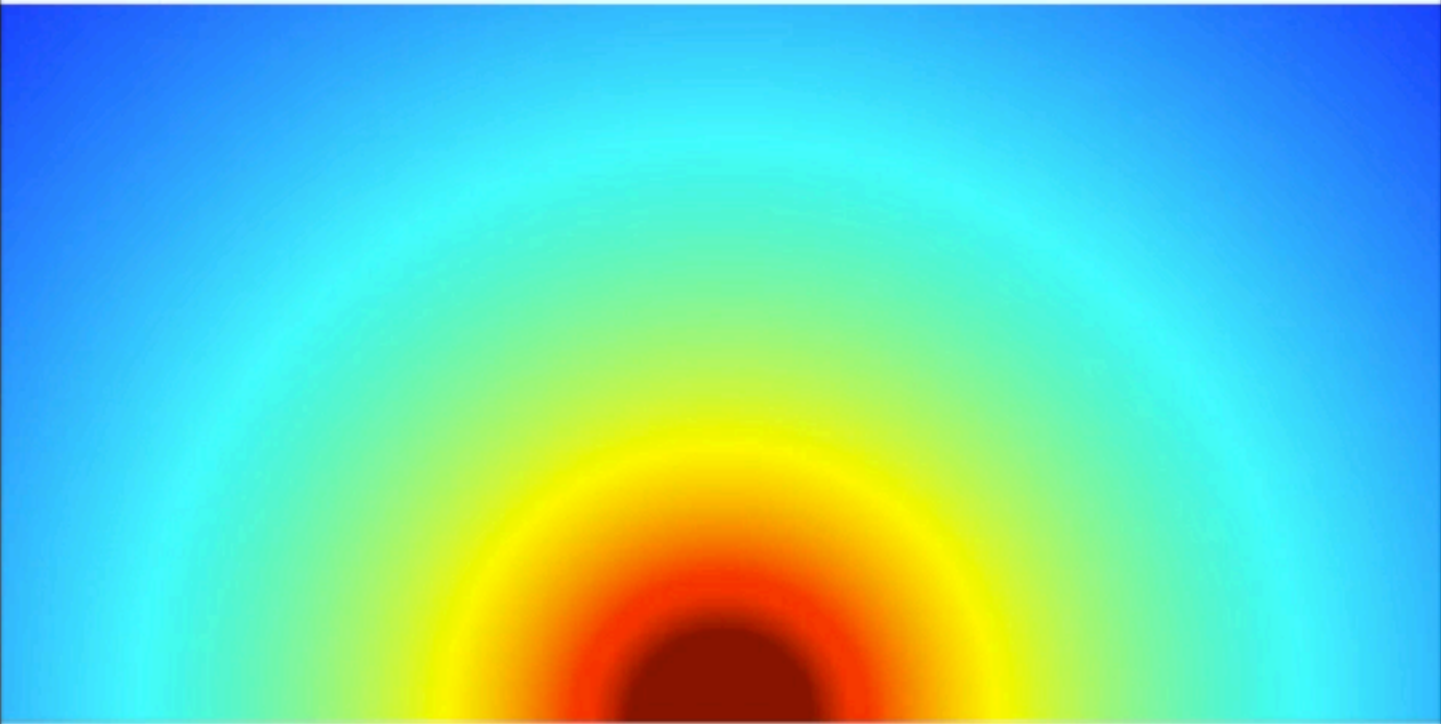
Bipolar Jets



Mechanical AGN feedback in Galaxy Clusters

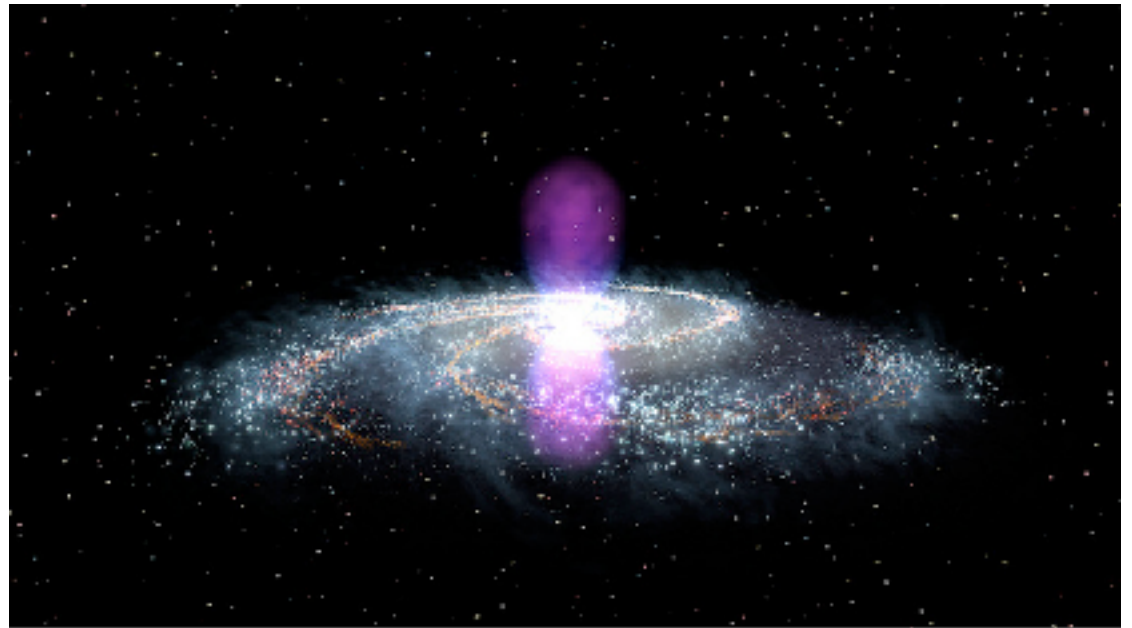
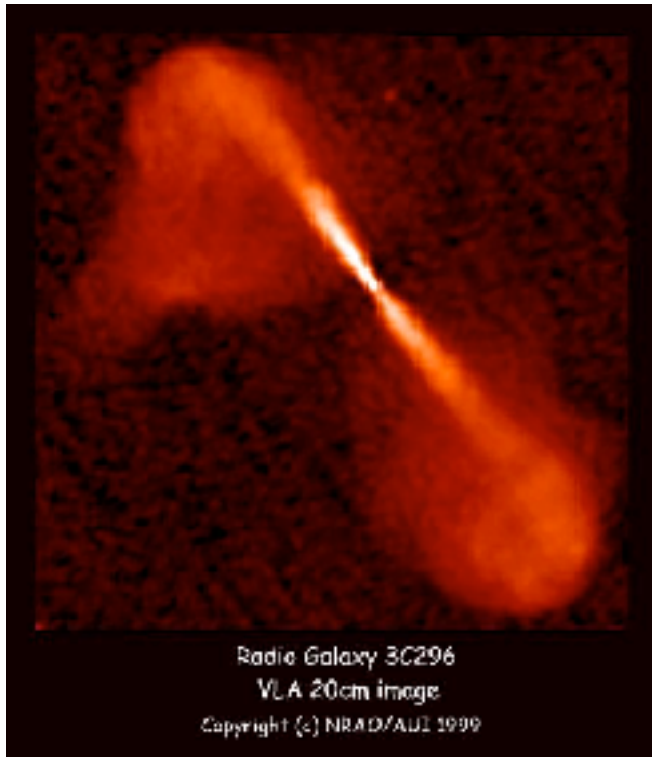
(Guo et al 2018, MNRAS; Duan & Guo 2018 & 2020, ApJ)

237Myr



Inner 200kpc

How did the MW story start?

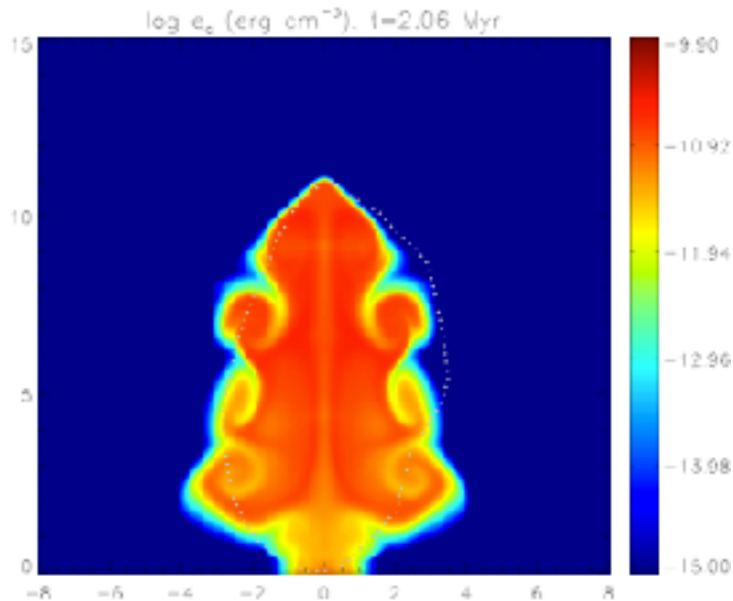


Fermi Bubbles

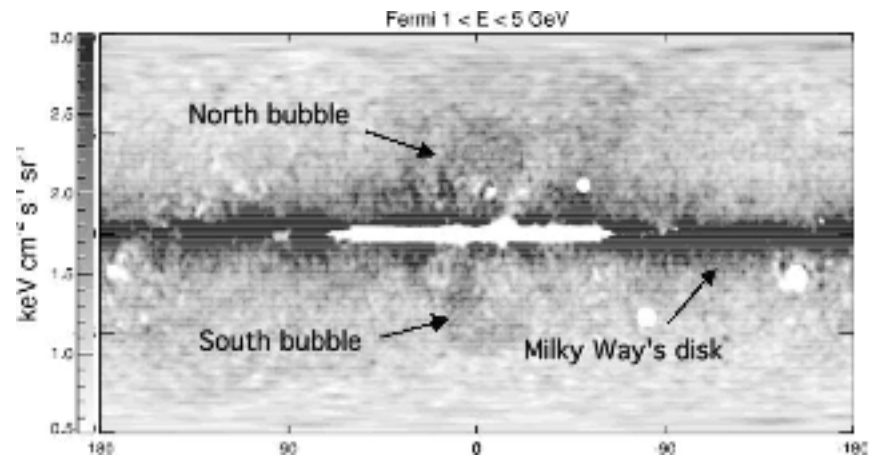
The AGN Jet Model of the Fermi bubbles (Guo & Mathews 2012)

A recent jet event reproduces many bubble features: location, size, shape, sharp edges

CR particle distribution

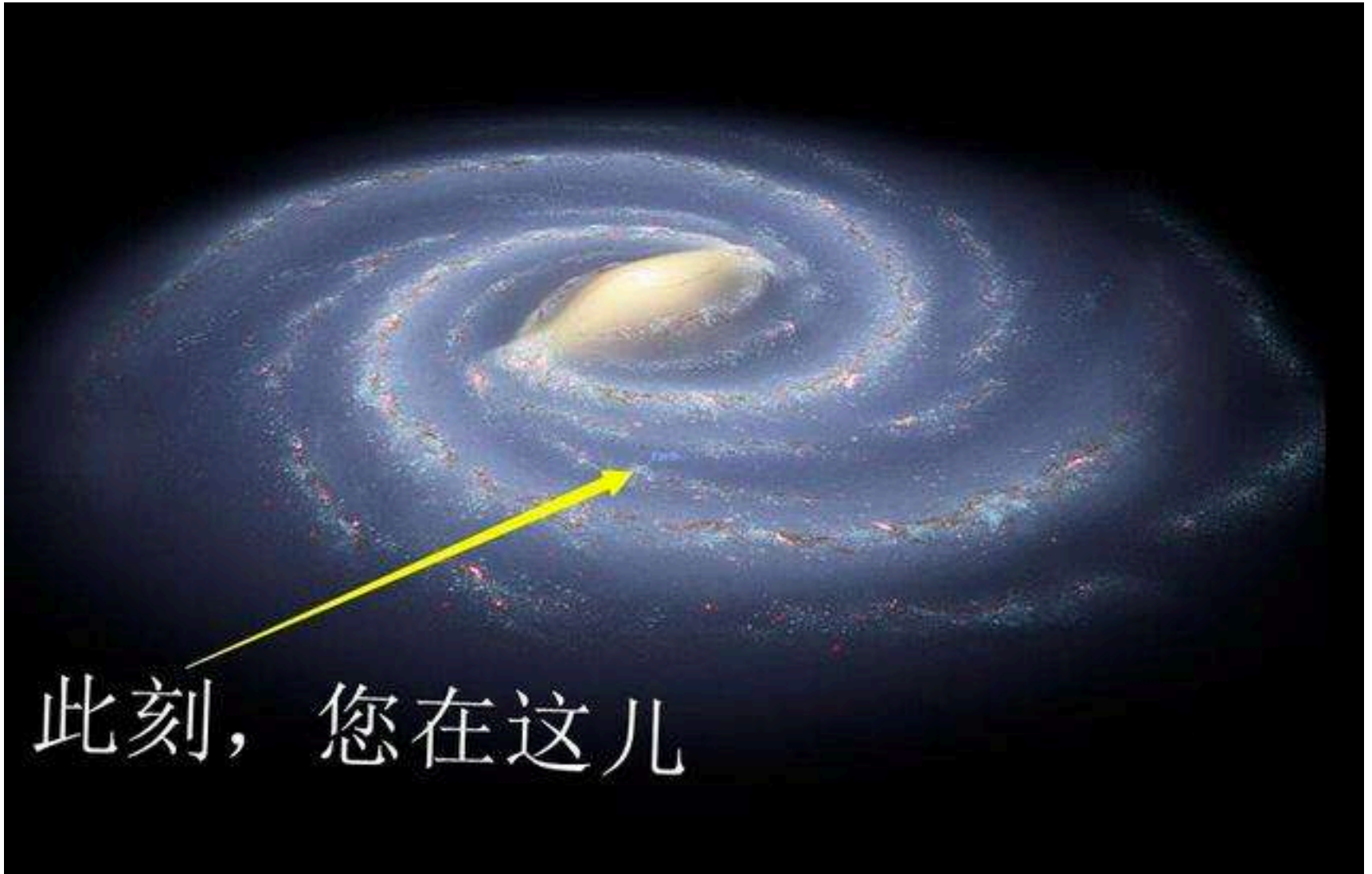


Guo & Mathews 2012

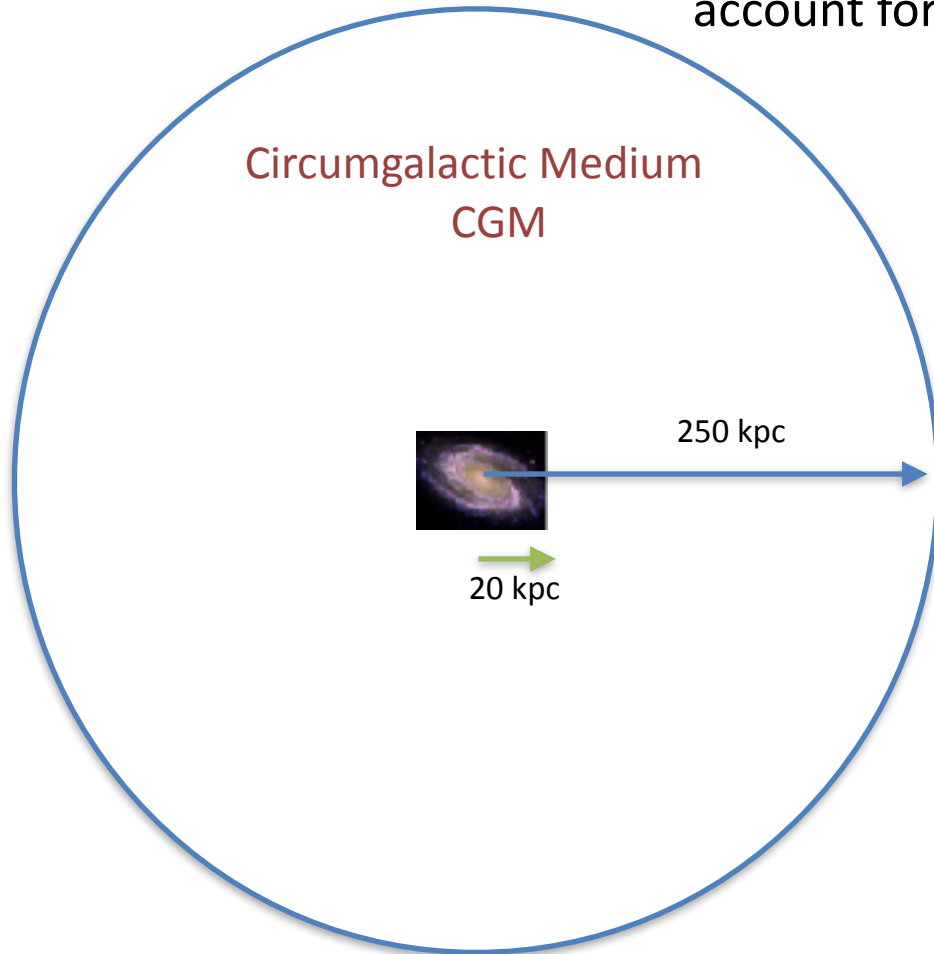


Su, Slatyer, and Finkbeiner, 2010

Our Galaxy: The Milky Way



The CGM may solve the missing baryon problem
The observed baryons in a typical galaxy only account for <20% of the baryonic allotment!



CGM: within virial radius of the galaxy, but beyond the disk and ISM

Problems: Galaxy Formation in LCDM

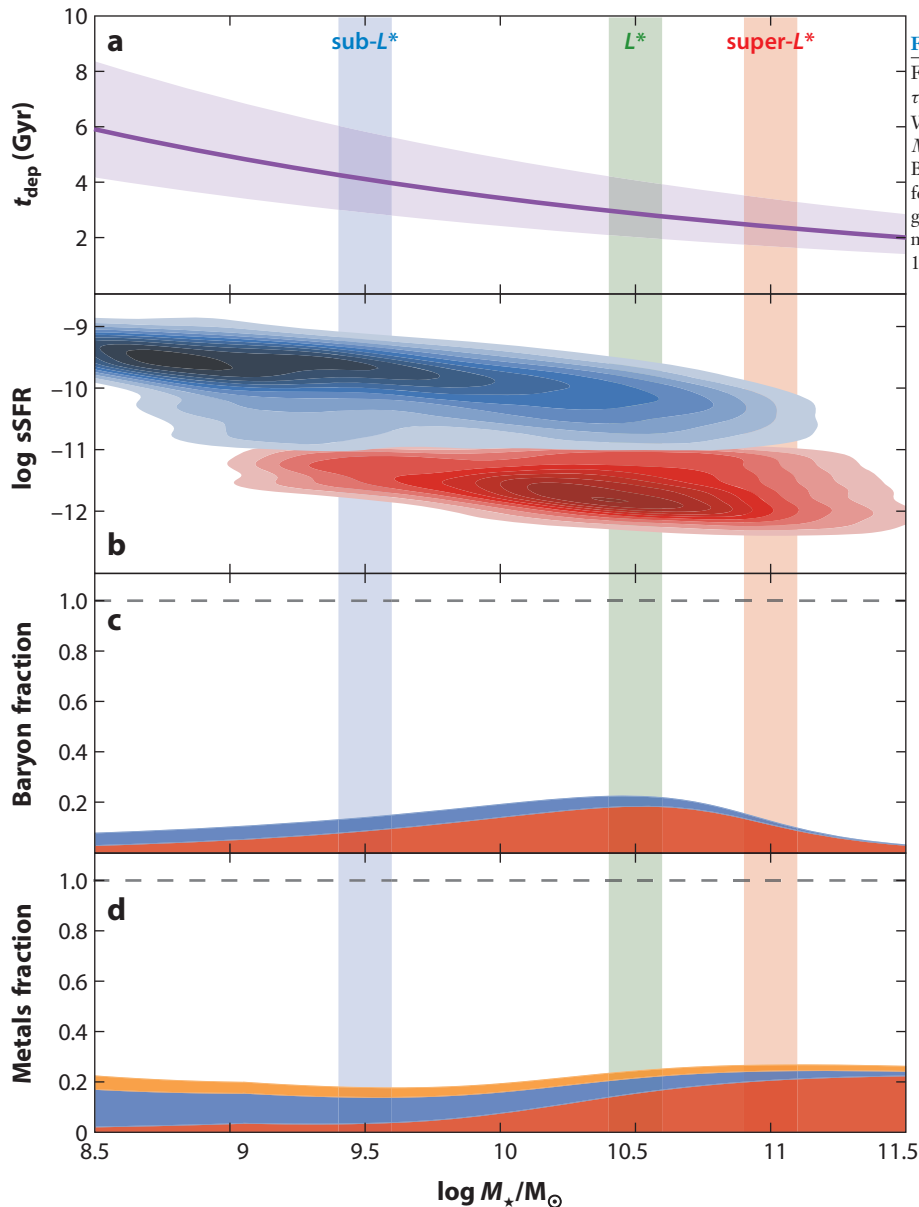


Figure 2

Four important problems in galaxy evolution viewed with respect to M_* . (a) The gas depletion timescale $\tau_{\text{dep}} \sim M_{\text{gas}}/\dot{M}_{\text{sfr}}$ for star-forming galaxies at $z \sim 0$, with M_{gas} from Peebles et al. (2014) and \dot{M}_{sfr} from Whitaker et al. (2012); the shading denotes ± 0.15 dex scatter in \dot{M}_{sfr} . (b) The galaxy bimodality in terms of M_* and specific SFR (Schiminovich et al. 2010). (c) The galactic baryon fraction, $M_*/[(\Omega_b/\Omega_m)M_{\text{halo}}]$ from Behroozi et al. (2010), with stars in red and interstellar gas in blue. (d) The “retained metals fraction,” metals for several galactic components relative to all the metals a galaxy has produced, with stars in red, interstellar gas in blue, and interstellar dust in orange. Adapted from Peebles et al. (2014) with permission. Vertical bars mark the properties of sub- L^* , L^* , and super- L^* galaxies at $\log M_*/M_\odot = 9.5$ (blue), 10.5 (green), and 11.0 (red), respectively. Abbreviation: SFR, star-formation rate.

Tumlinson et al 2017

Stars and AGNs are major energy sources for the heating, ionization, enrichment of IGM, ICM, and CGM, which also in turn affect galaxy formation.

The Hot Halo Gas in the Milky Way

ON A POSSIBLE INTERSTELLAR GALACTIC CORONA*

LYMAN SPITZER, JR.

Princeton University Observatory

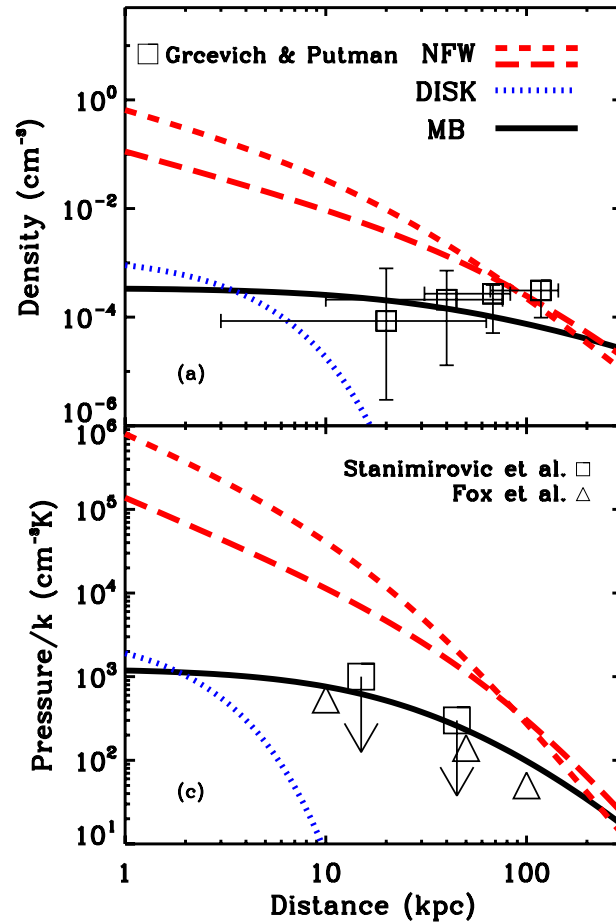
Received March 24, 1956

ABSTRACT

The physical conditions in a possible interstellar galactic corona are analyzed. Pressure equilibrium between such a rarefied, high-temperature gas and normal interstellar clouds would account for the existence of such clouds far from the galactic plane and would facilitate the equilibrium of spiral arms in the presence of strong magnetic fields. Observations of radio noise also suggest such a corona.

At a temperature of 10^6 degrees K, the electron density in the corona would be $5 \times 10^{-4}/\text{cm}^3$; the extension perpendicular to the galactic plane, 8000 pc; the total number of electrons in a column perpendicular to the galactic plane, about $2 \times 10^{19}/\text{cm}^2$; the total mass, about $10^8 M_{\odot}$. The mean free path would be 4 pc, but the radius of gyration even in a field of 10^{-15} gauss would be a small fraction of this. Such a corona is apparently not observable optically except by absorption measures shortward of 2000 Å.

Evidence for Hot Halo Gas in the Milky Way

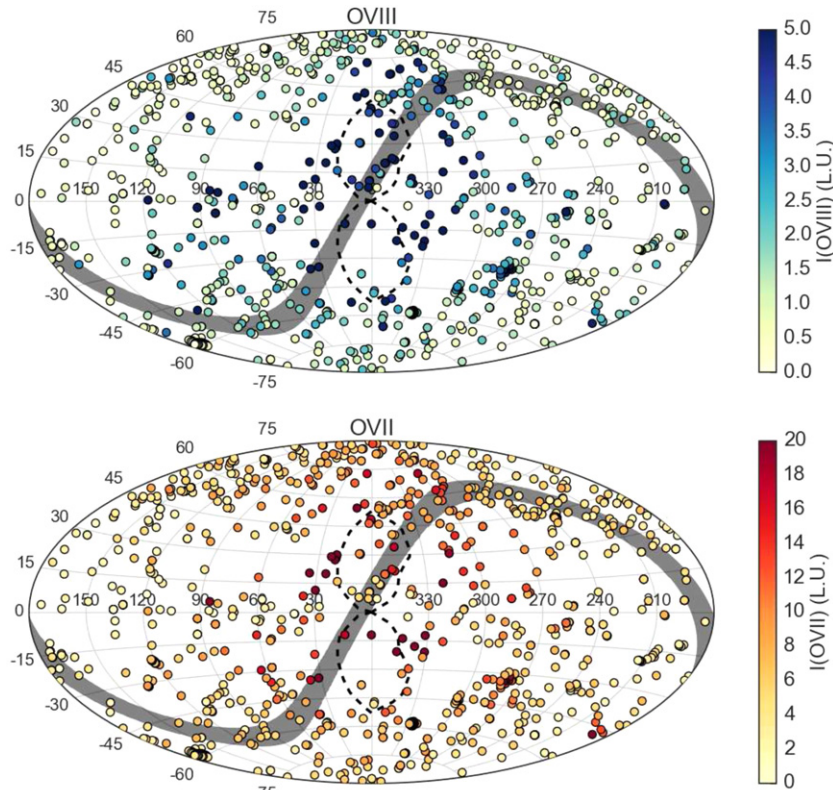


ram-pressure stripping

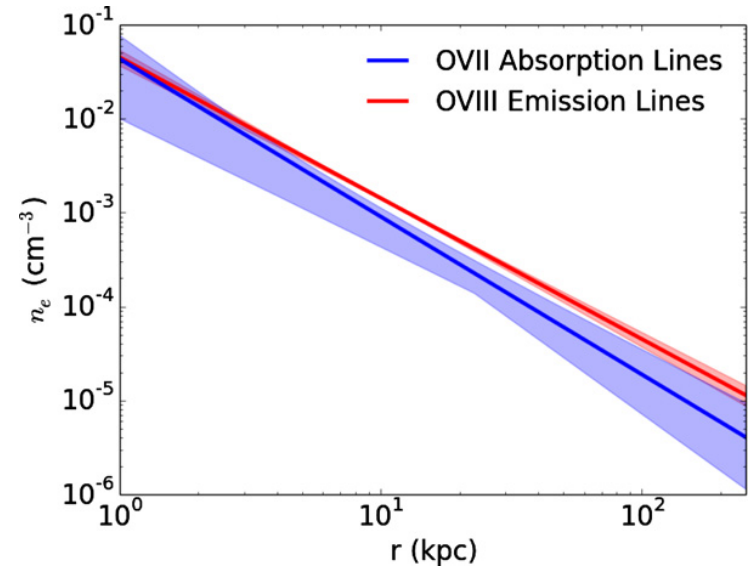
HVC pressure confinement

Fang et al 2013

Evidence for Hot Halo Gas in the Milky Way



O VII and VIII emission line strength



beta-mode fit for the hot CGM

$$\rho_\beta(r) \approx \frac{\rho_b r_c^{3\beta}}{r^{3\beta}},$$

$$: (\rho \propto r^{-1.5})$$

Miller & Bregman 2015

A Physically-Motivated CGM Model

$$\rho(r) = \frac{\rho_0}{(r + r_1)^\alpha (r + r_2)^{3-\alpha}},$$

$r_1 = 3r_s/4$ (inner core from cosmological simulations)

$r_2 = r_s$ cored-NFW profile

$r_2 = 100, 200, 300$ kpc; impact of feedback

gas distribution in the halo is expected to have $r_2 > r_s$. Our density distribution is relatively flat at $r \ll r_1$, and scales roughly as $\rho \propto r^{-1}$ at $r_1 \ll r \ll r_2$. At sufficiently large radii $r \gg r_2$, the gas density distribution approaches to the reduced NFW distribution: $\rho(r) \propto r^{-3}$, guaranteeing that distant regions are not substantially affected by feedback processes.

Hydrostatic Equilibrium w/ Non-thermal Pressure Support

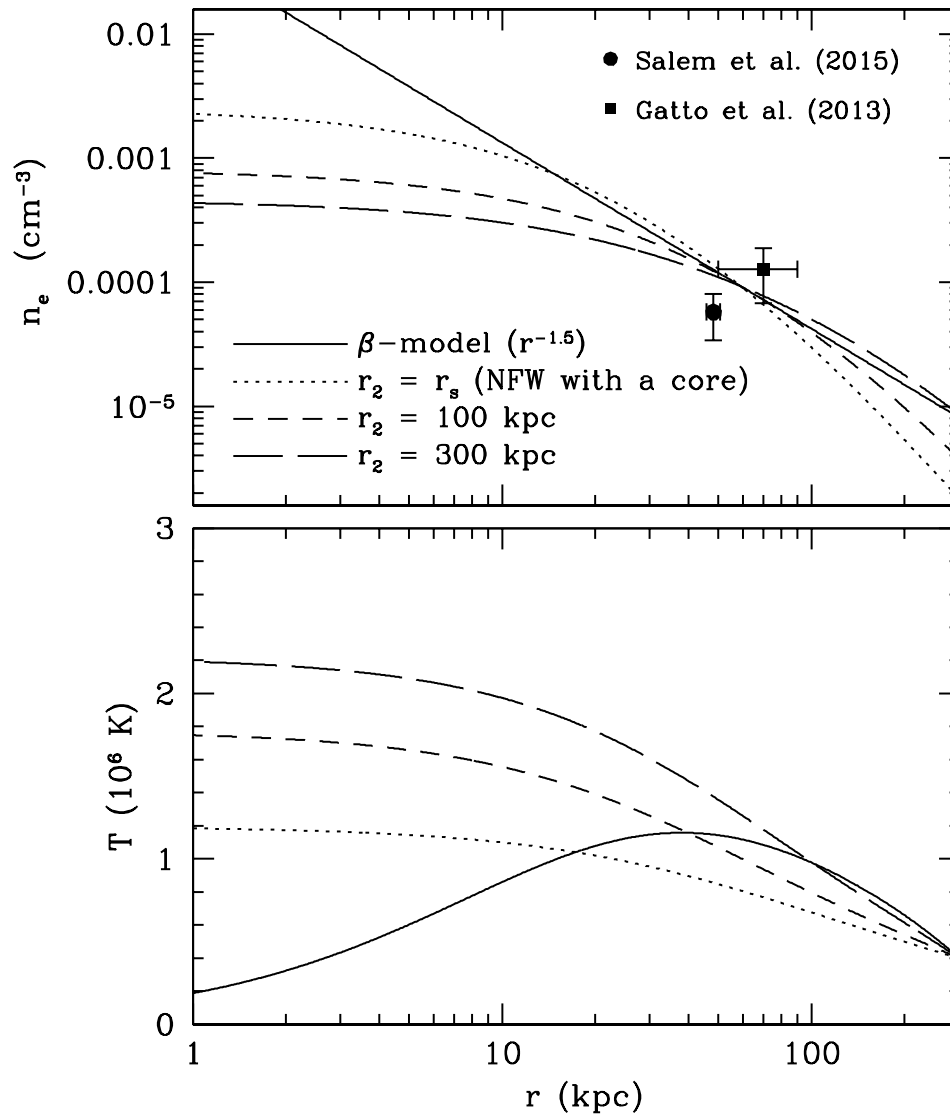
$$dP/dr = -(1-f_{\text{nt}})G\rho M(< r)/r^2$$

$$-\frac{d \ln T}{d \ln r} - \frac{d \ln \rho}{d \ln r} = (1 - f_{\text{nt}}) \frac{\mu m_{\mu}}{k_B T} \frac{GM(< r)}{r}$$

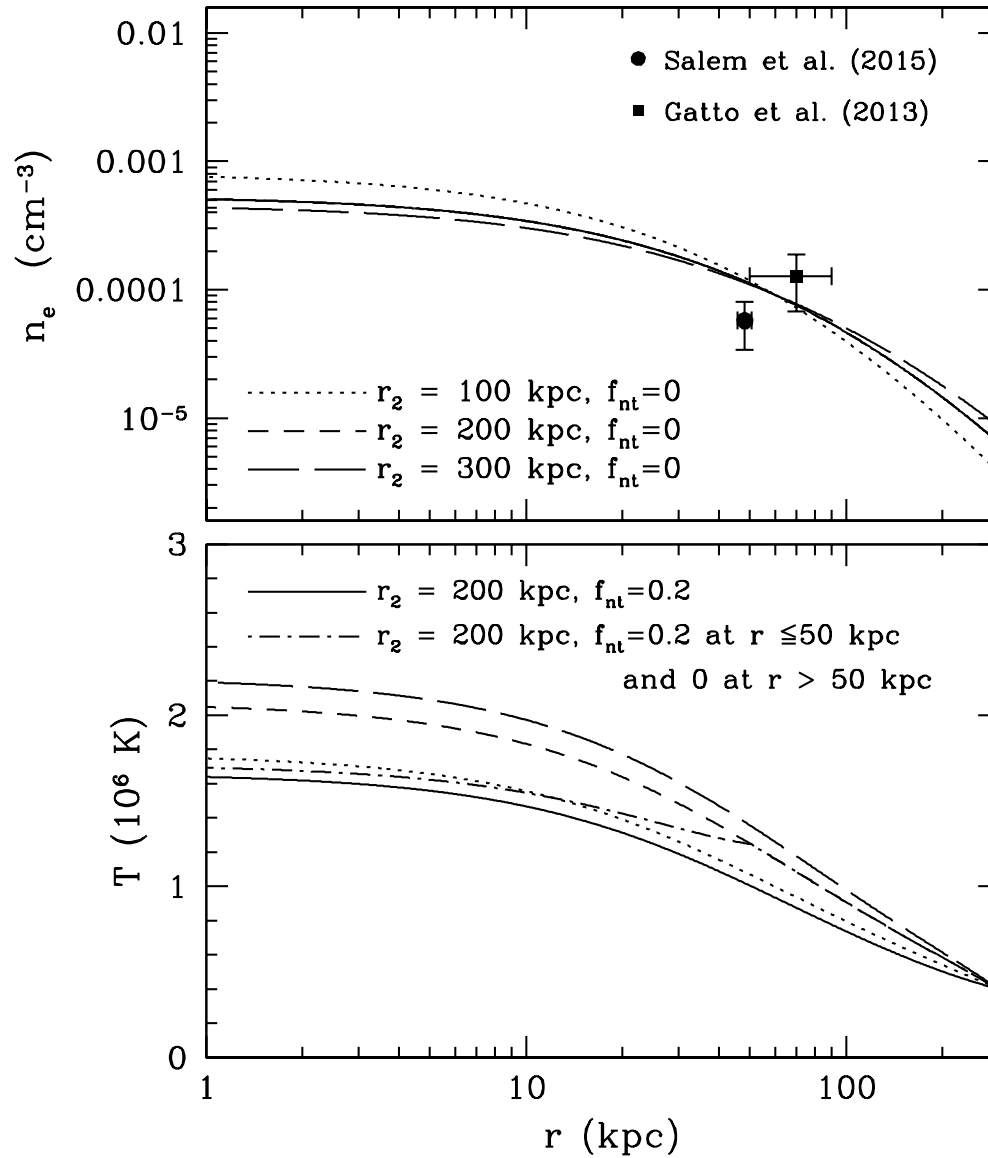
The virial temperature at the virial radius $\sim 5 \times 10^5 (M_{\text{vir}}/10^{12} M_{\odot})^{2/3} \text{ K}$

$$\rho(r) = \frac{\rho_0}{(r + r_1)^{\alpha}(r + r_2)^{3-\alpha}},$$

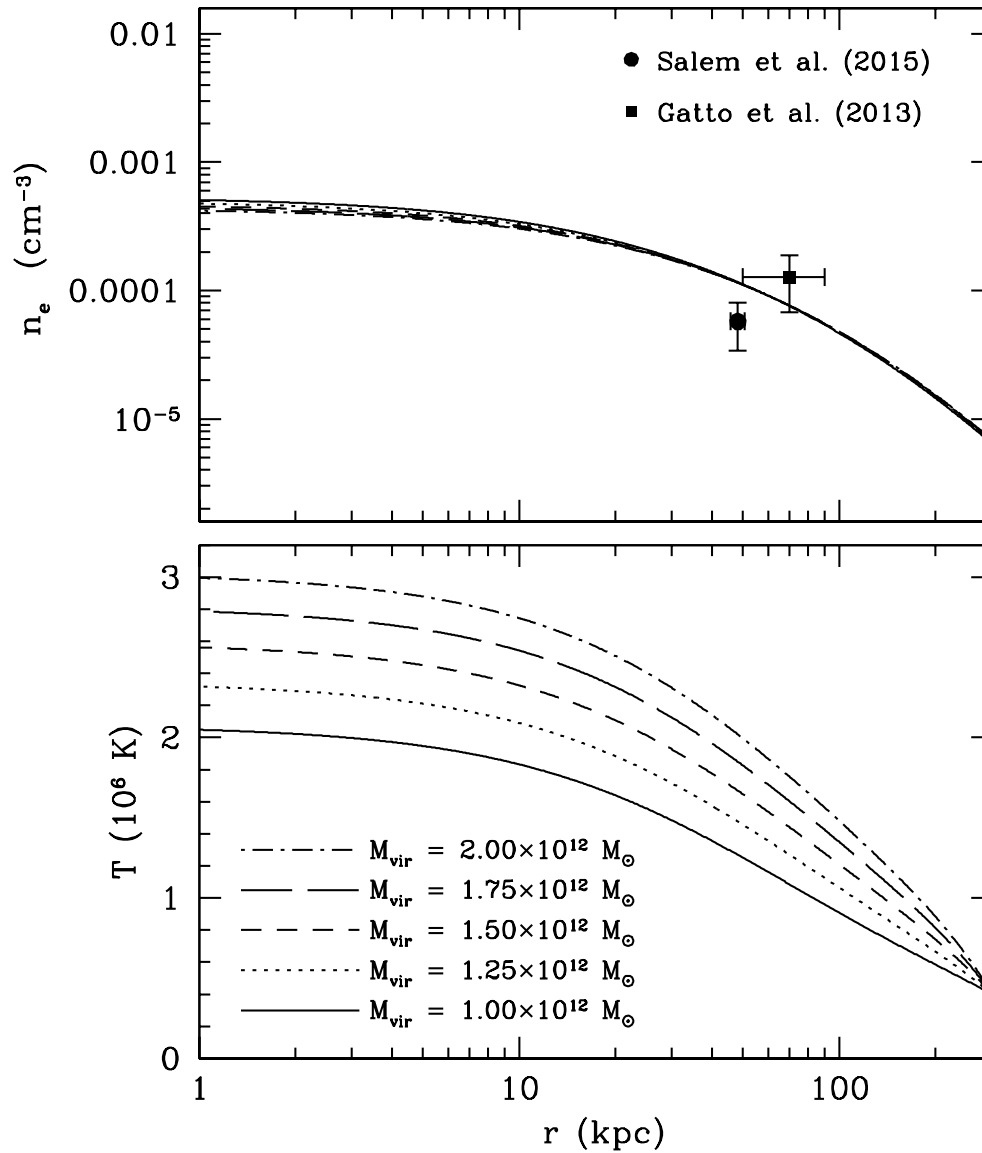
Our Models



Our Models



Dependence on the halo mass



Hydrostatic Equilibrium w/ Non-thermal Pressure Support

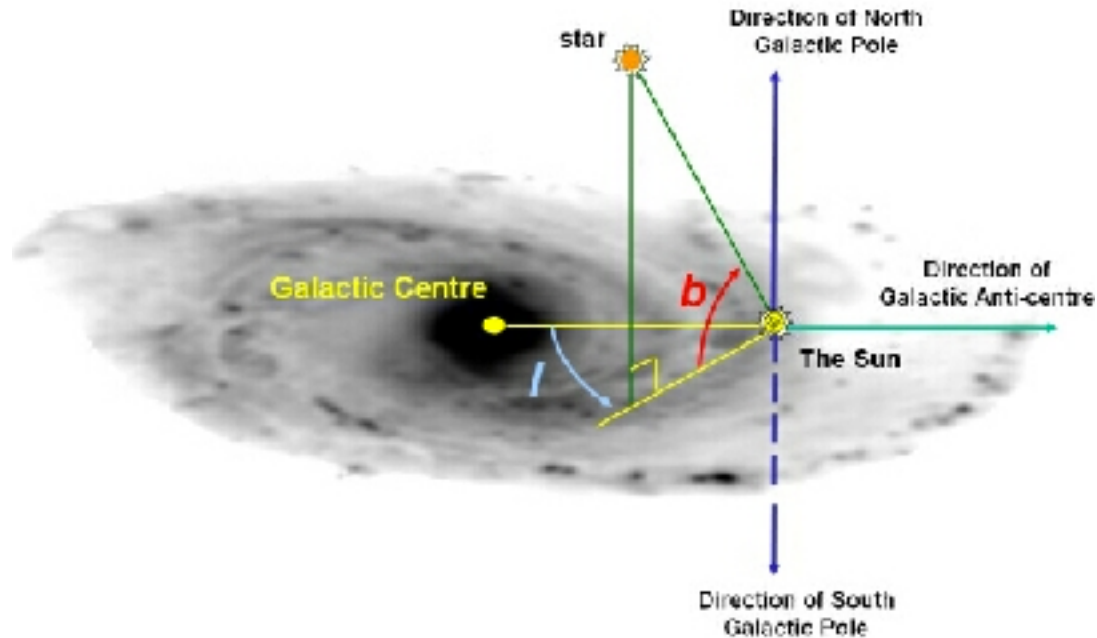
$$dP/dr = -(1-f_{\text{nt}})G\rho M(< r)/r^2$$

$$-\frac{d \ln T}{d \ln r} - \frac{d \ln \rho}{d \ln r} = (1 - f_{\text{nt}}) \frac{\mu m_{\mu}}{k_B T} \frac{GM(< r)}{r}$$

The virial temperature at the virial radius $\sim 5 \times 10^5 (M_{\text{vir}}/10^{12} M_{\odot})^{2/3} \text{ K}$

$$\rho(r) = \frac{\rho_0}{(r + r_1)^{\alpha} (r + r_2)^{3-\alpha}},$$

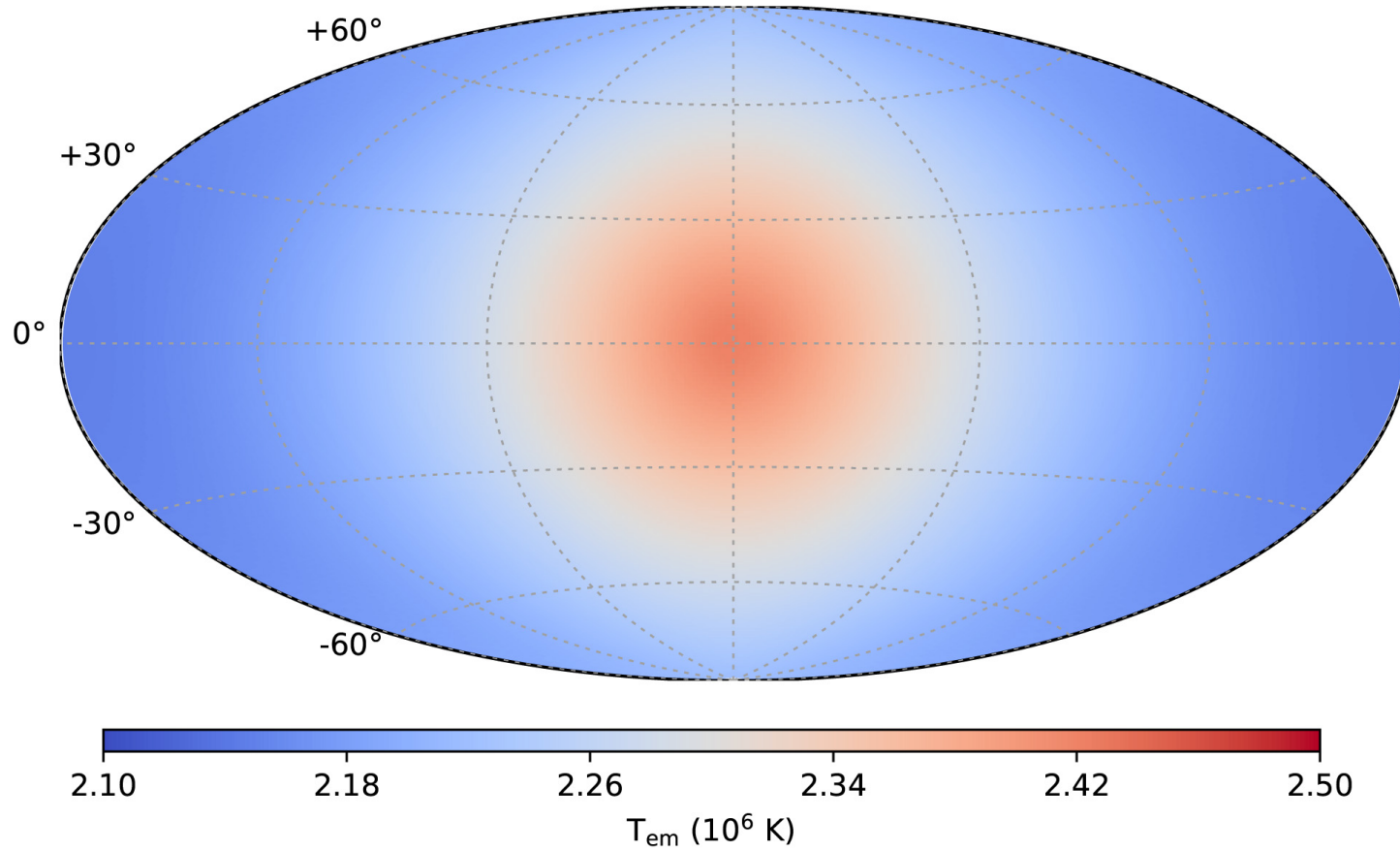
Observed halo gas temperature

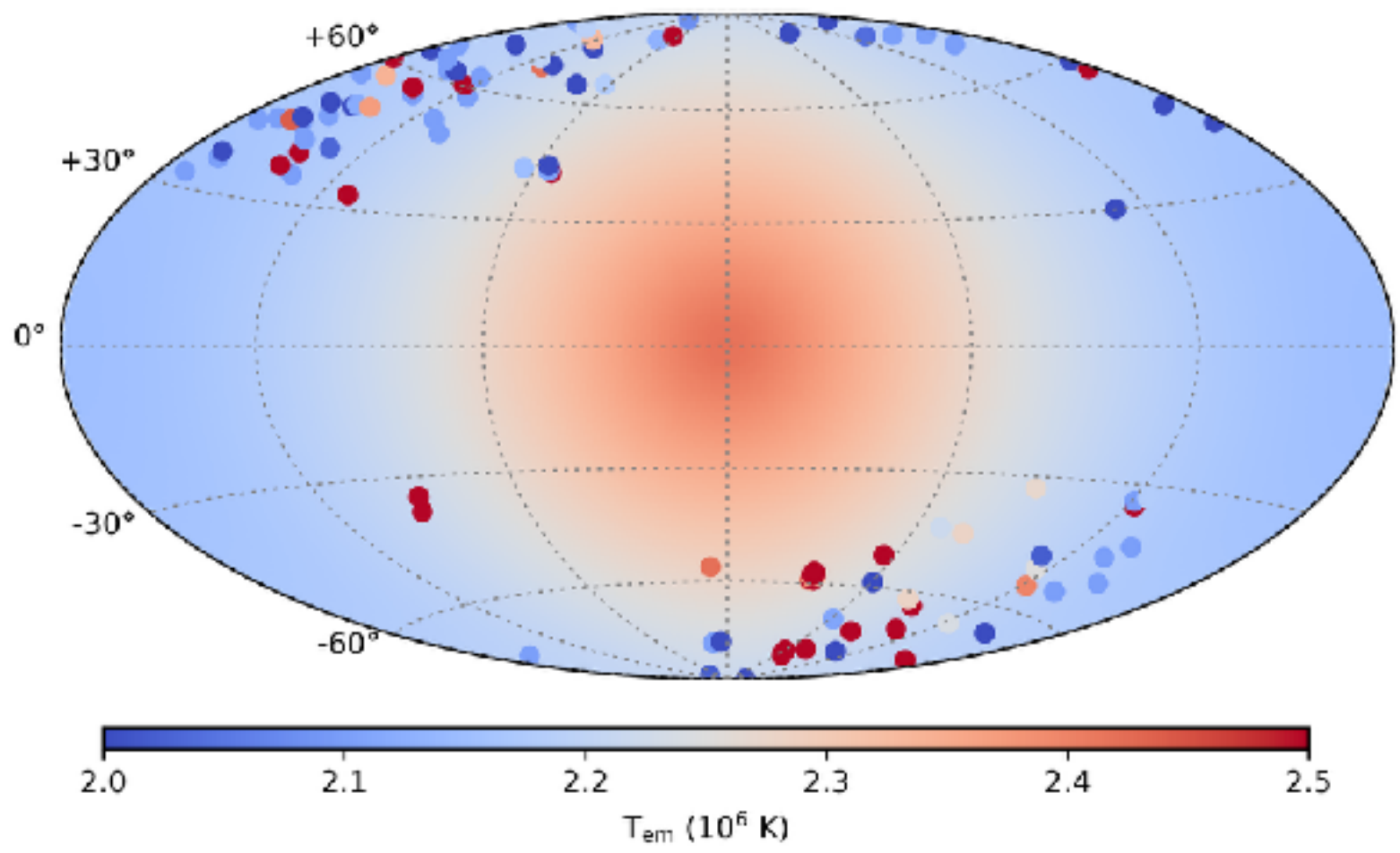


$$T_{\text{em}}(l, b) = \frac{\int_{\text{los}} n_e n_H T \epsilon(T, Z) dR}{\int_{\text{los}} n_e n_H \epsilon(T, Z) dR},$$

where $\epsilon(T, Z)$ is the 0.5 – 2.0 keV X-ray emissivity of the hot gas,

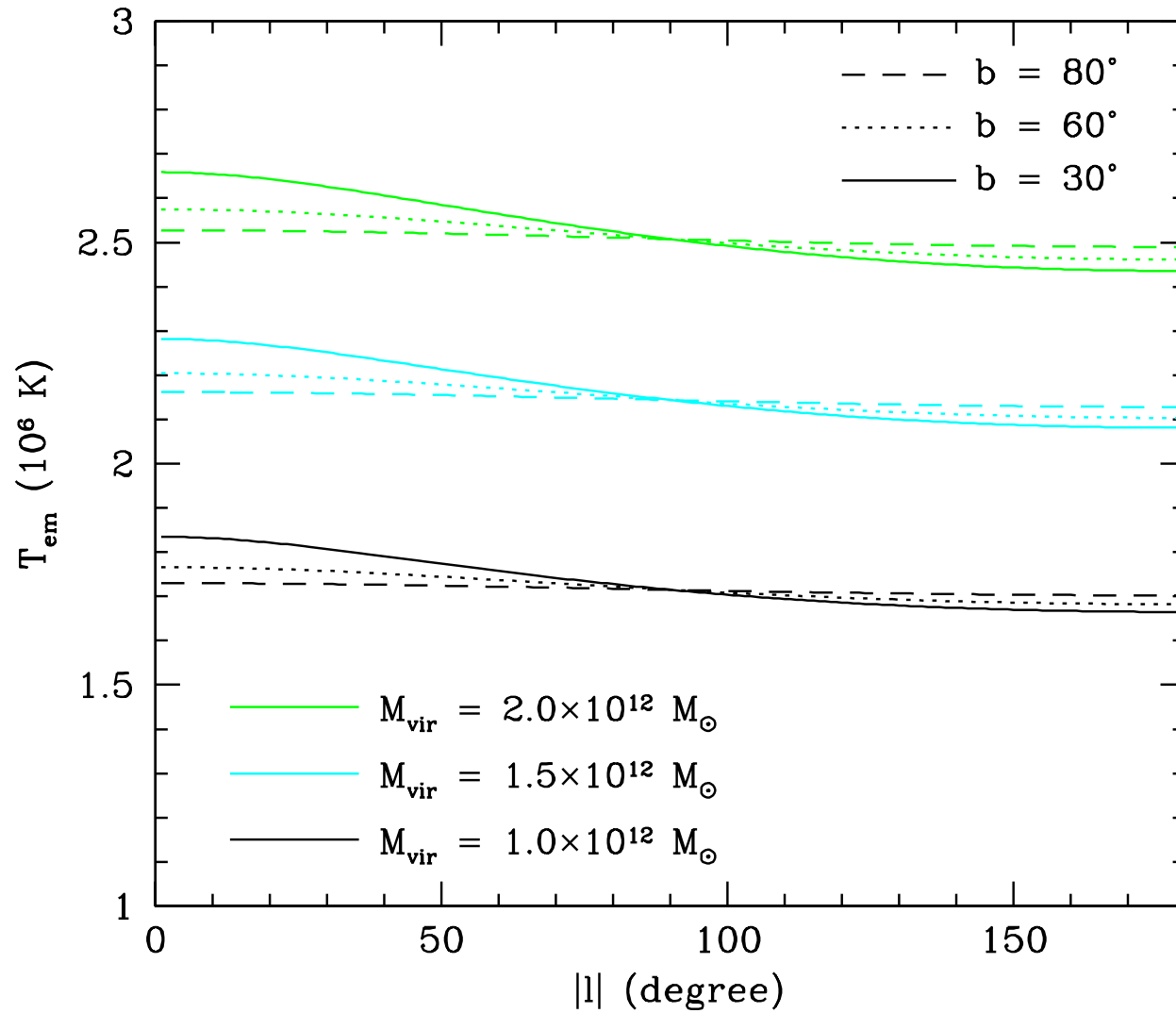
Predicted halo gas temperature



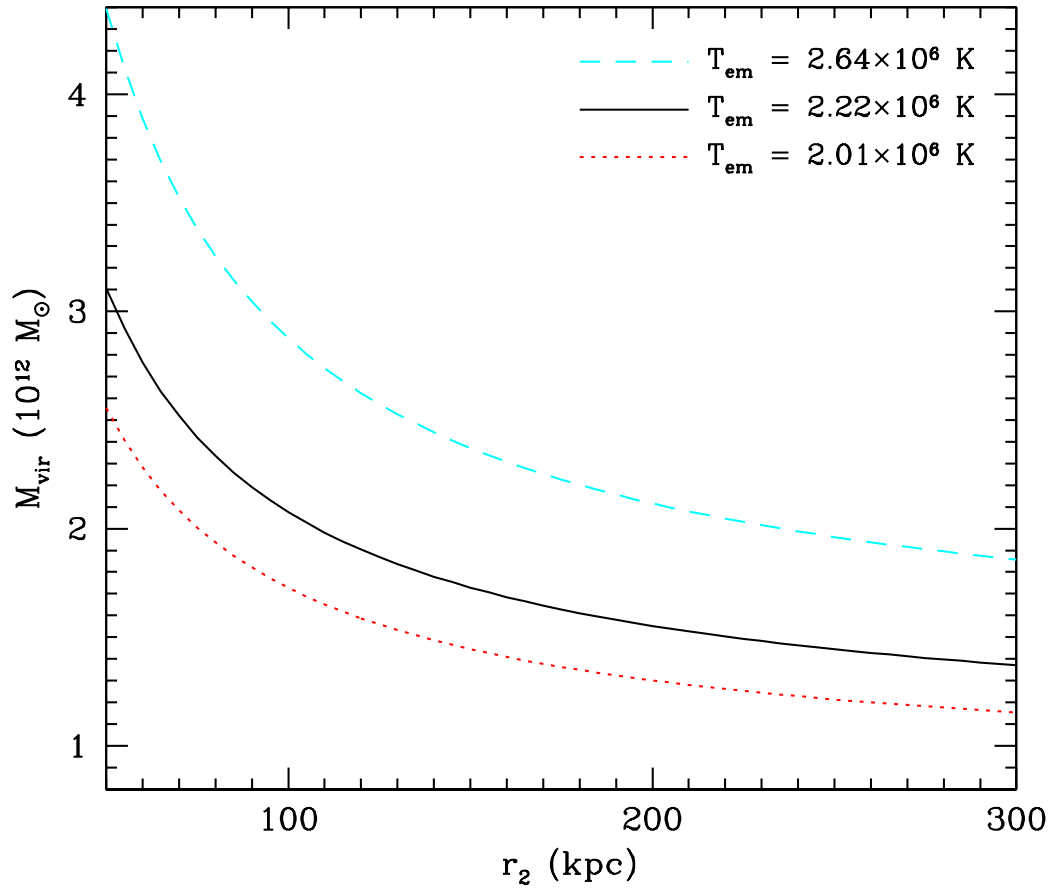


Guo et al, 2020; Data from XMM-Newton observations (Henley & Shelton 2013)

Dependence on the halo mass



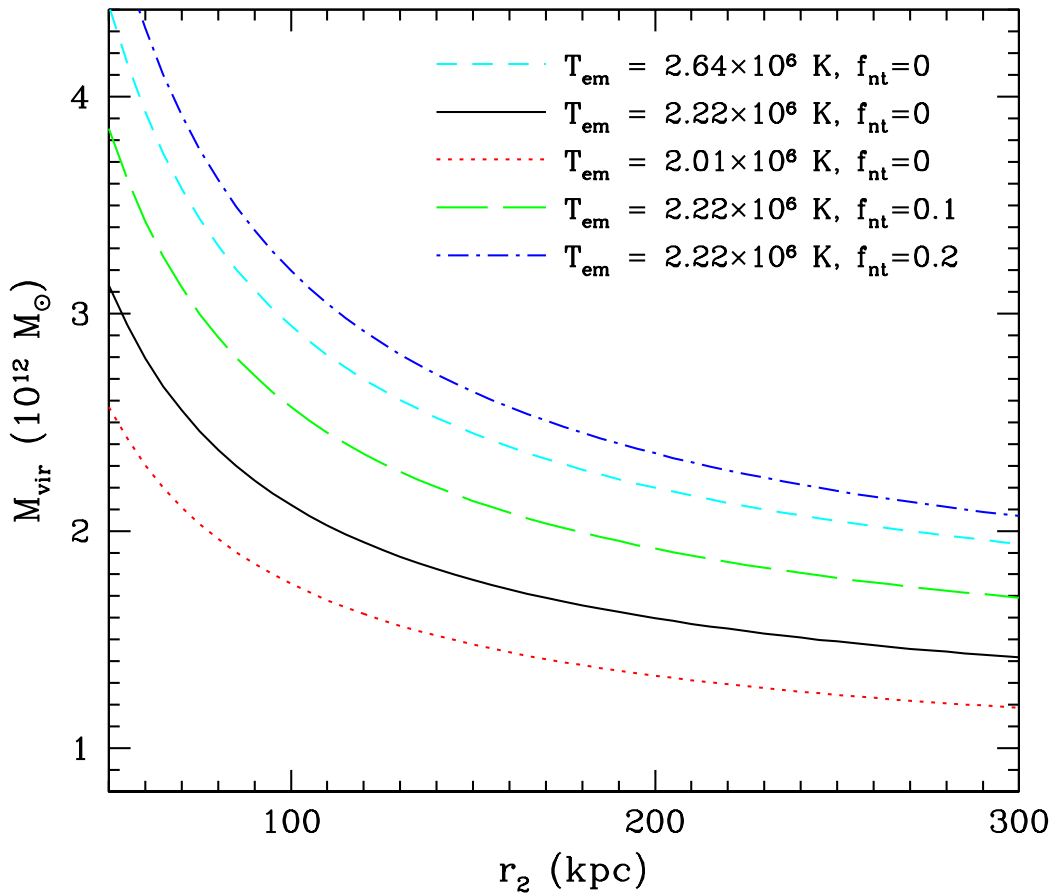
Constraints on the halo mass



$$M_{\text{vir}} = 1.60^{+1.35}_{-0.41} \times 10^{12} M_{\odot}$$

($f_{\text{nt}} = 0$)

Constraints on the halo mass

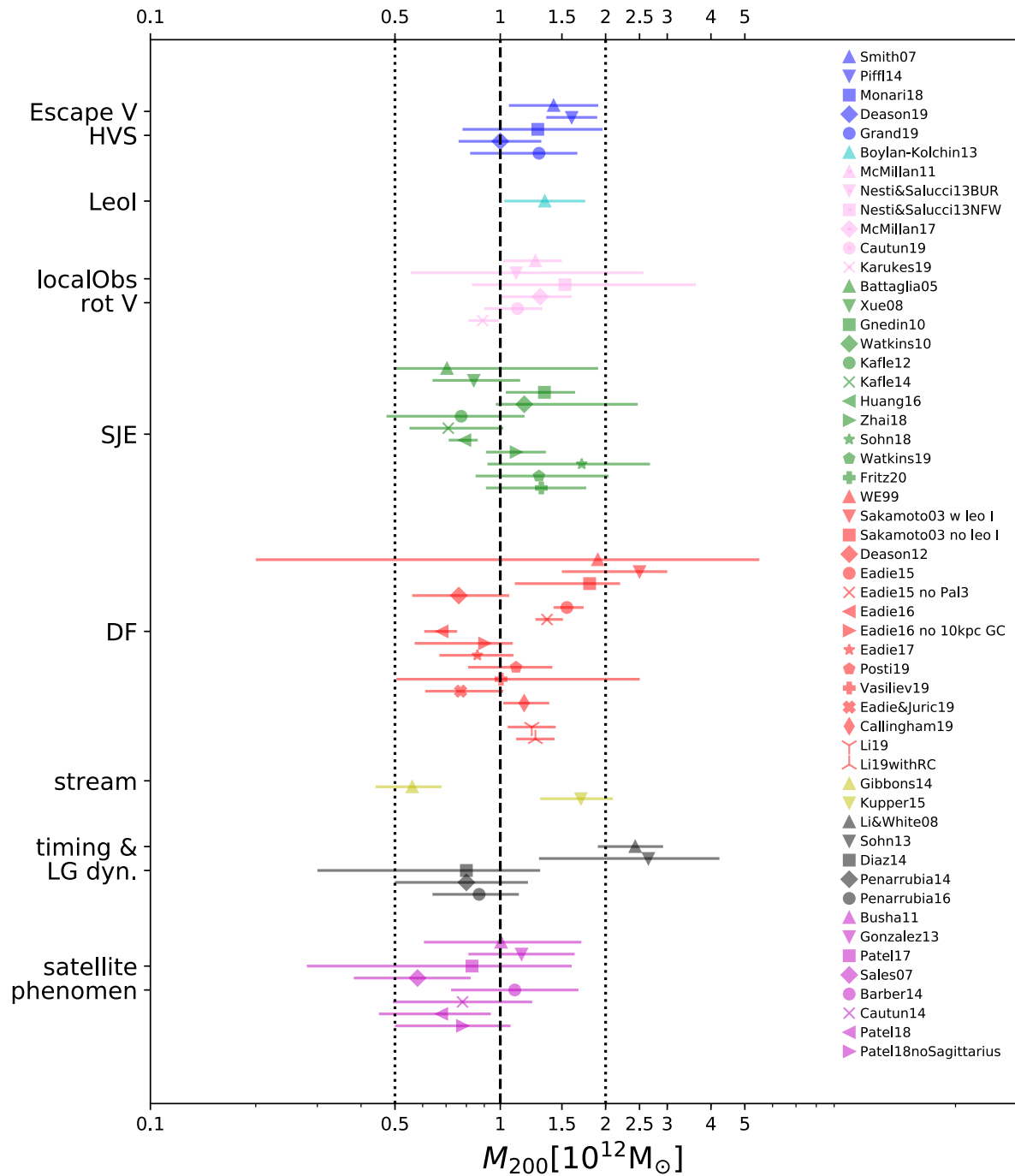


$$M_{\text{vir}} = 1.60^{+1.35}_{-0.41} \times 10^{12} M_{\odot}$$

$(f_{\text{nt}} = 0)$

$$M_{\text{vir}} = 1.92^{+1.66}_{-0.51} \times 10^{12} M_{\odot}$$

$(f_{\text{nt}} = 0.1)$

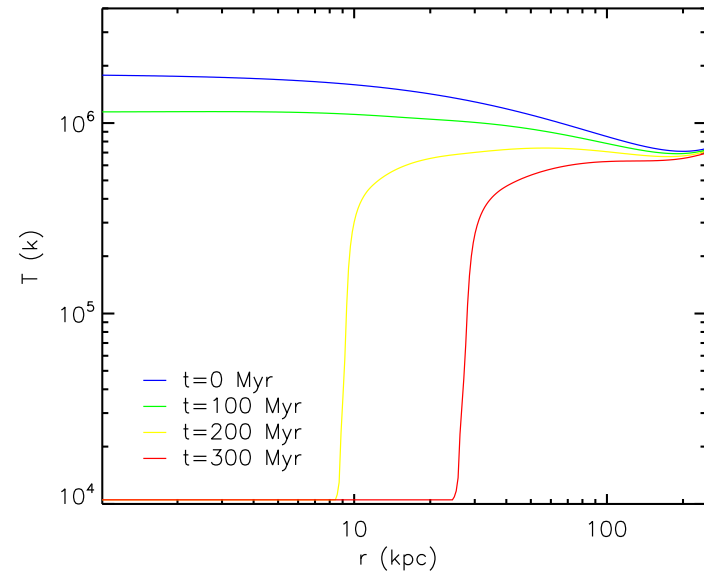
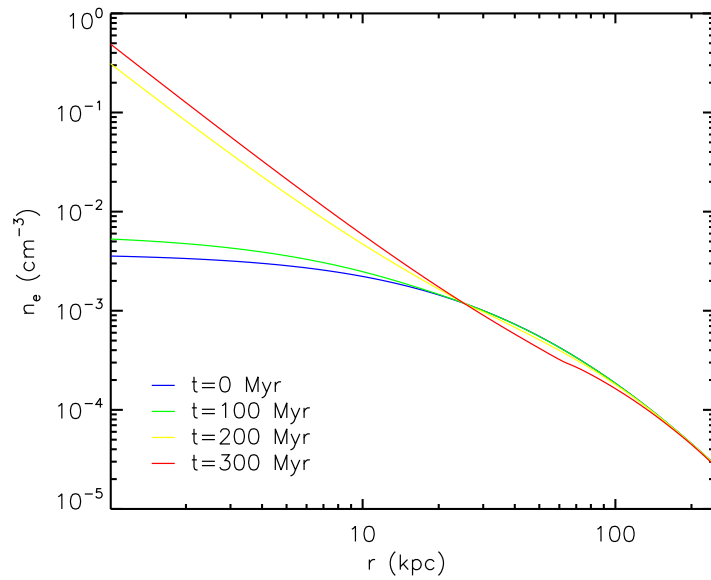


Wang et al 2020

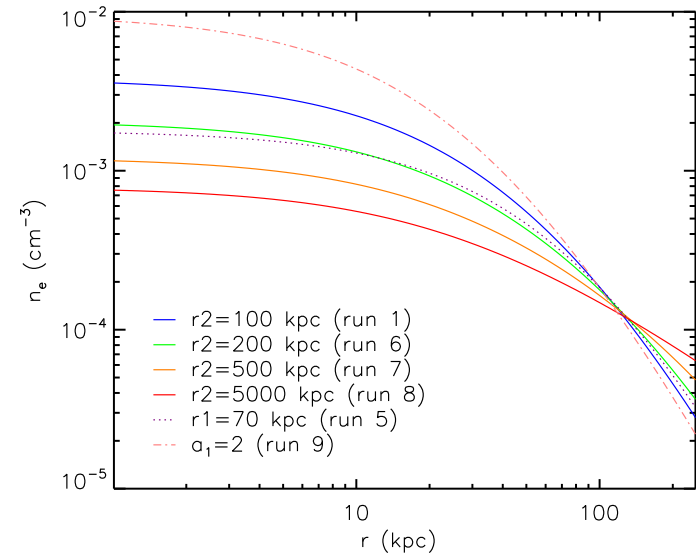
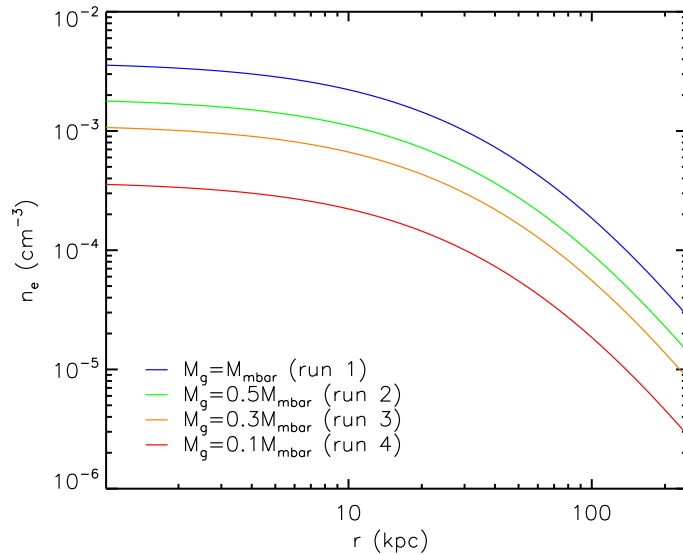
$$M_{\text{vir}} = 1.60^{+1.35}_{-0.41} \times 10^{12} M_{\odot}$$

Guo et al, 2020

cooling flows in the CGM

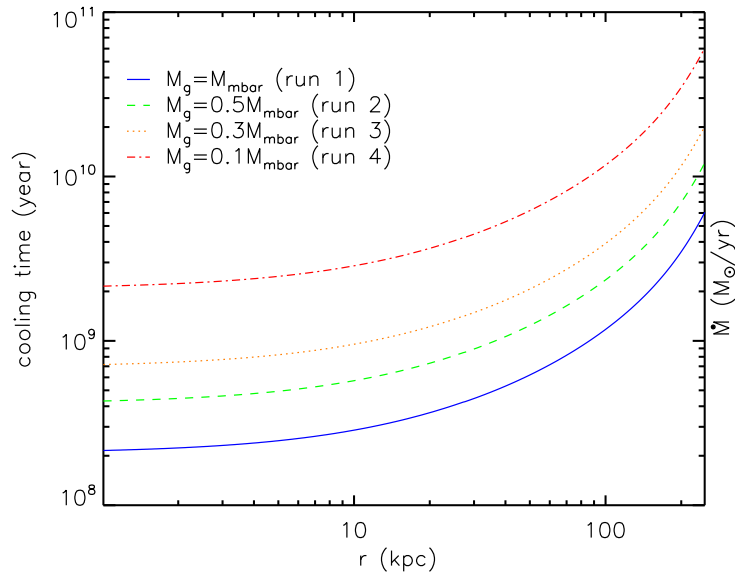


Dependence on the CGM density distribution

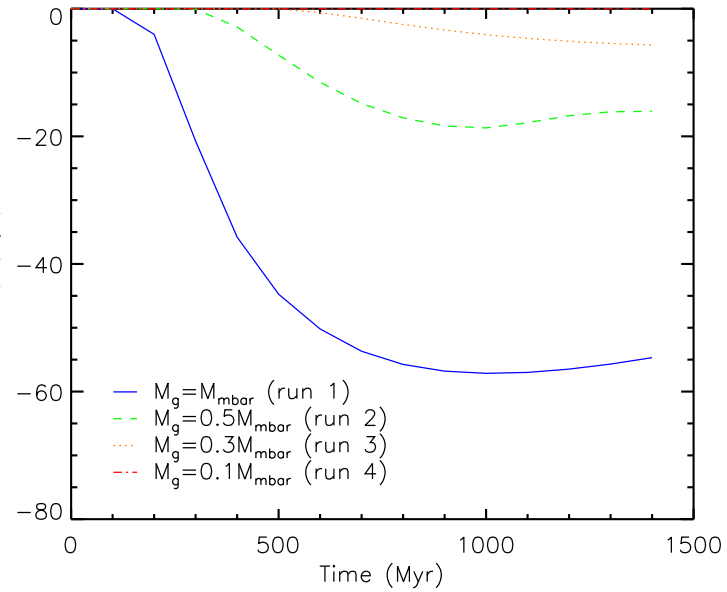


$$\rho(r) = \frac{\rho_0}{(r + r_1)^\alpha (r + r_2)^{3-\alpha}},$$

Dependence on the halo gas mass



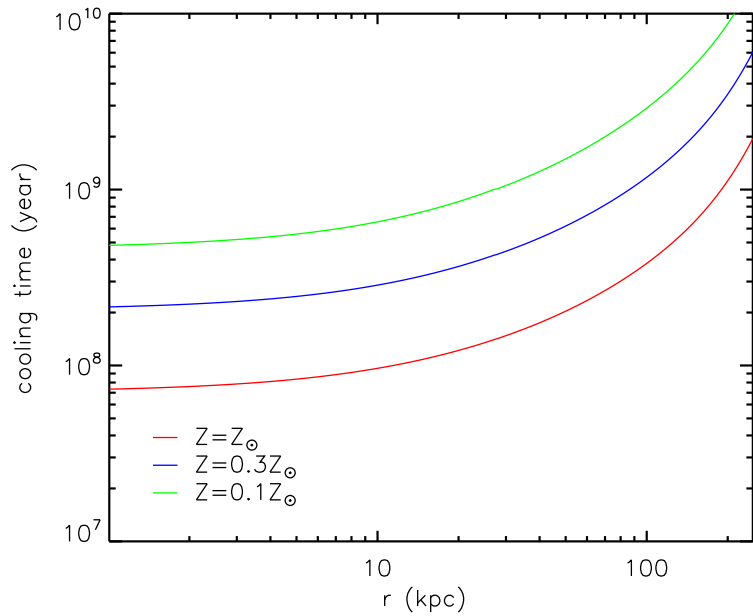
cooling time



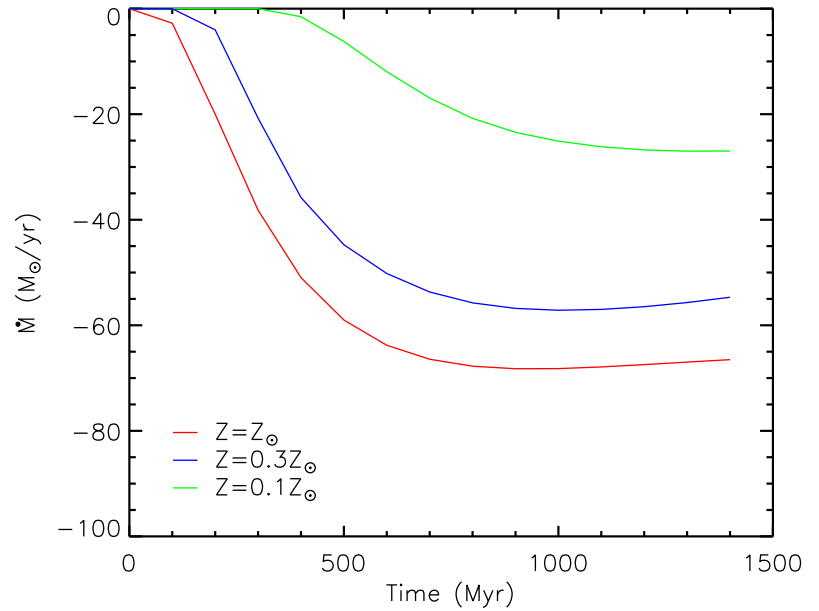
Mass inflow rate vs time

$$\rho(r) = \frac{\rho_0}{(r + r_1)^\alpha (r + r_2)^{3-\alpha}},$$

Dependence on the gas metallicity

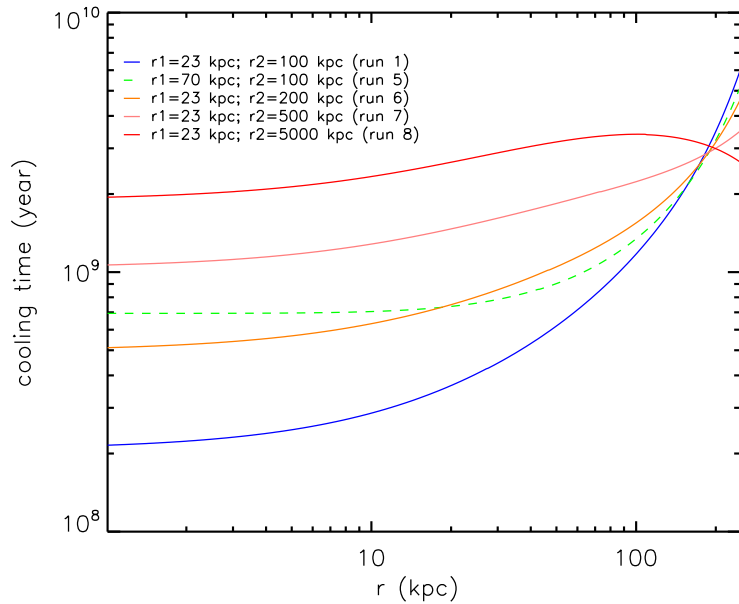


cooling time

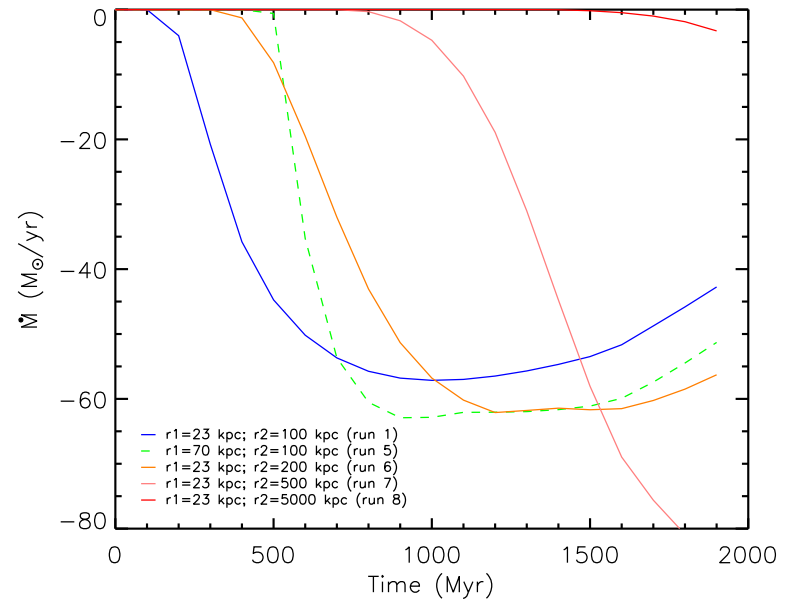


Mass inflow rate vs time

Dependence on the halo gas distribution



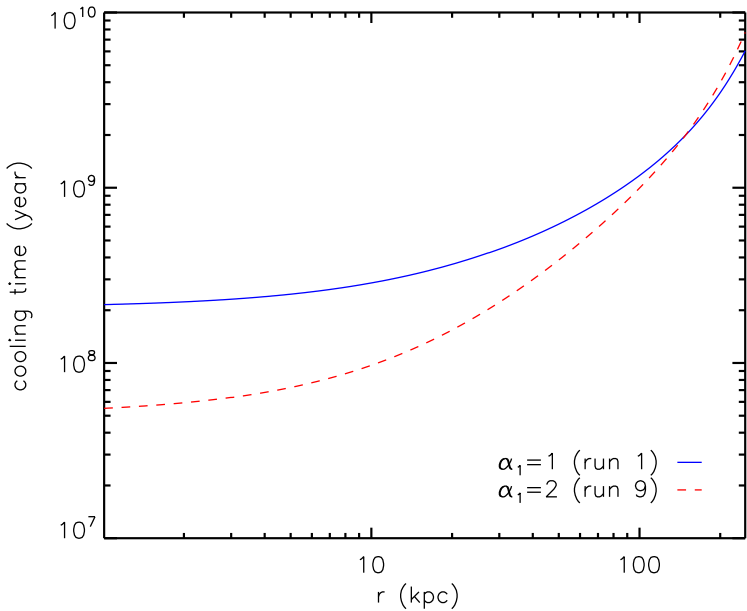
cooling time



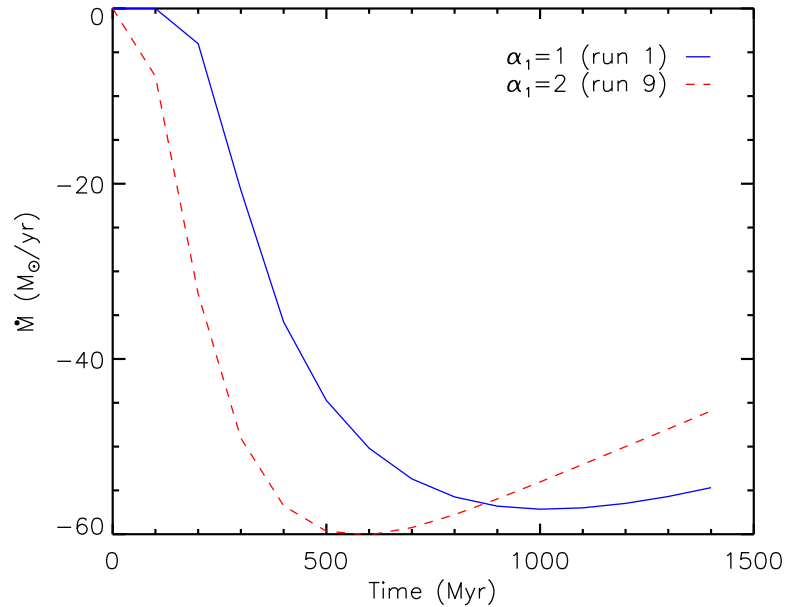
Mass inflow rate vs time

$$\rho(r) = \frac{\rho_0}{(r + r_1)^\alpha (r + r_2)^{3-\alpha}},$$

Dependence on the halo gas distribution



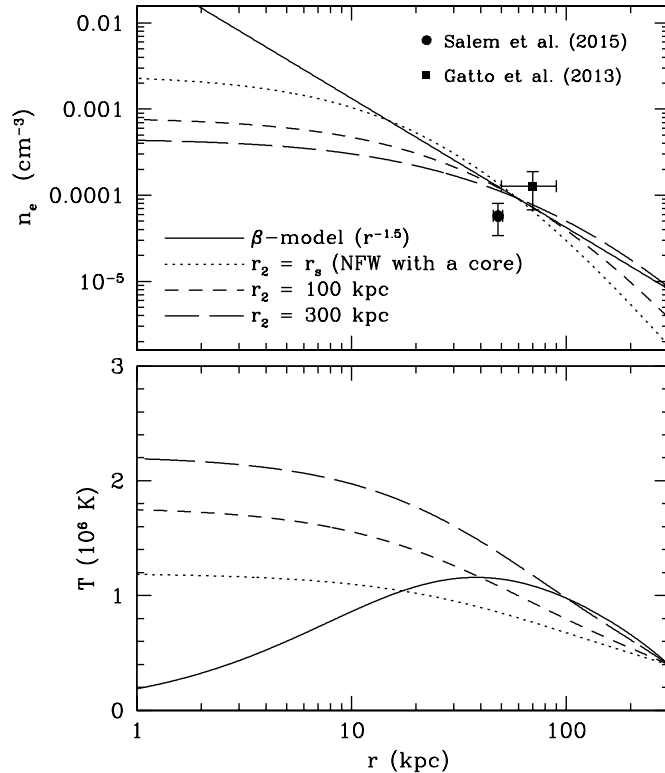
cooling time



Mass inflow rate vs time

$$\rho(r) = \frac{\rho_0}{(r + r_1)^\alpha (r + r_2)^{3-\alpha}},$$

Typical Mass Inflow Rate



$$\sim 5M_{\odot} \text{ yr}^{-1} \text{ to } \sim 60M_{\odot} \text{ yr}^{-1}$$

$$M_{\text{hot}} = 3.8 \times 10^{10} M_{\odot}$$

cooling rate $\sim 5 - 10$ solar mass per year

It is widely believed that the current observed SFR in the MW is about $1 - 2 M_{\odot} \text{ yr}^{-1}$ (Robitaille & Whitney 2010; Chomiuk & Povich 2011). Recent observations suggest that the bulk of the stars at the GC were formed at least 8 Gyr ago, and the star formation activity there was very quiescent during most times of the past 8 Gyr (Nogueras-Lara et al. 2019). The low

Cooling and Heating Rates

Cooling rate of CGM (0.3 solar metallicity):

$$9.46 \times 10^{40} \text{ erg/s when } M_g = 0.3M_{\text{mbar}}$$

$$2.63 \times 10^{41} \text{ erg/s when } M_g = 0.5M_{\text{mbar}}$$

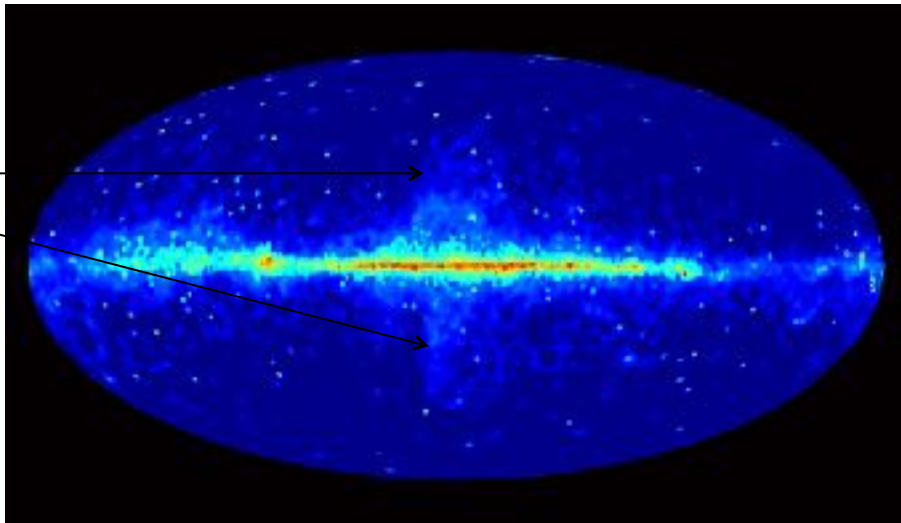
$$1.06 \times 10^{42} \text{ erg/s when } M_g = M_{\text{mbar}}$$

Supernova heating rate: $6.03 \times 10^{41} \text{ erg/s}$
(1.9 SN per century)

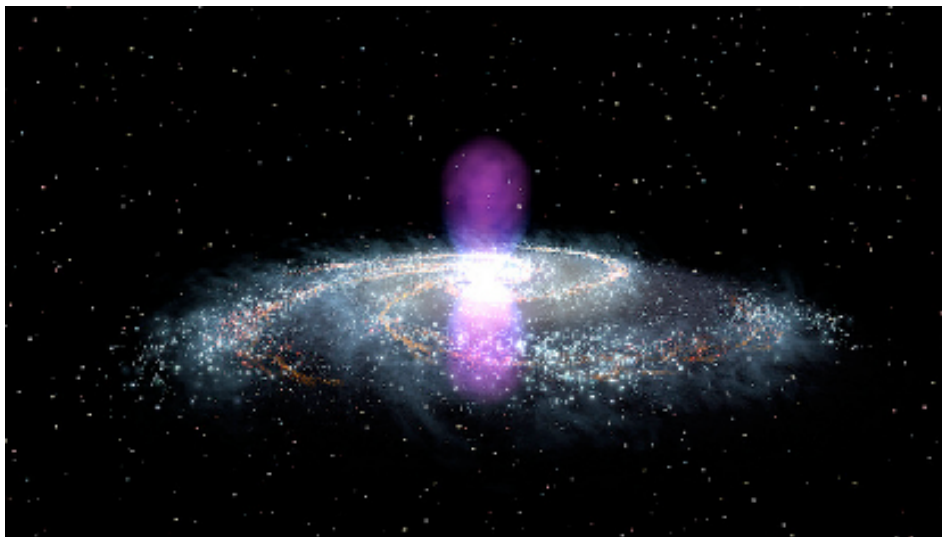
AGN feedback heating rate: ?

The Fermi Bubbles in the Milky Way

The Fermi bubbles!



The All-sky Fermi View at $E > 10$ GeV

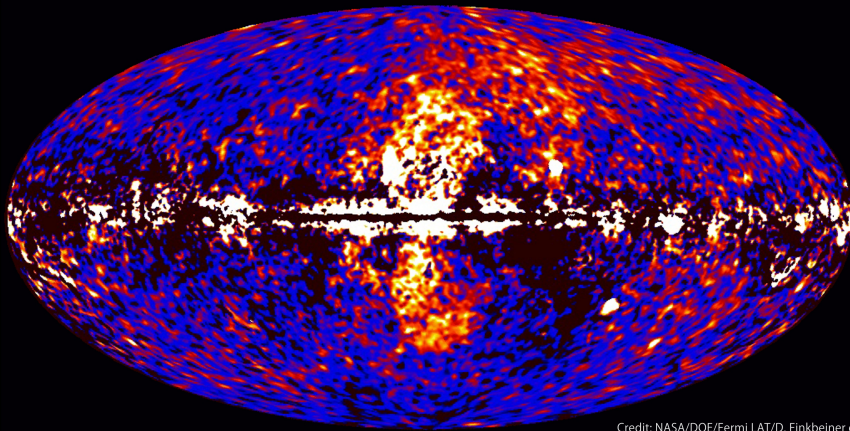


Artist's conception of Fermi Bubbles

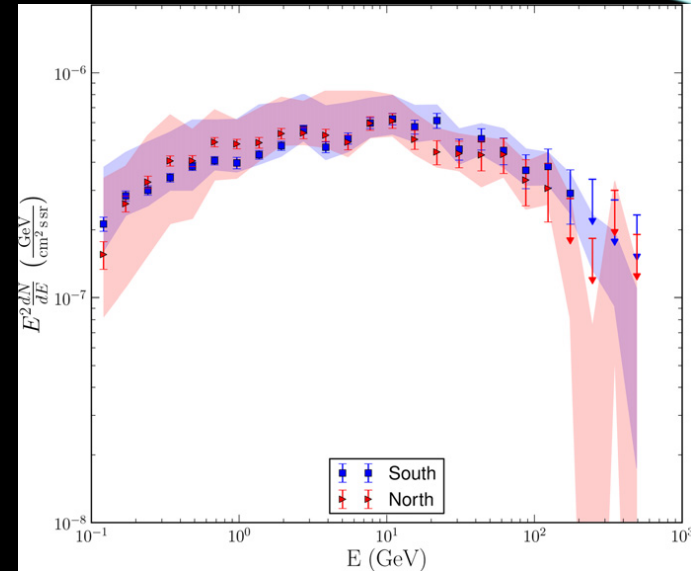
The Fermi Bubbles in the Milky Way

Observation

Fermi data reveals giant gamma-ray bubbles



Credit: NASA/DOE/Fermi LAT/D. Finkbeiner et al.



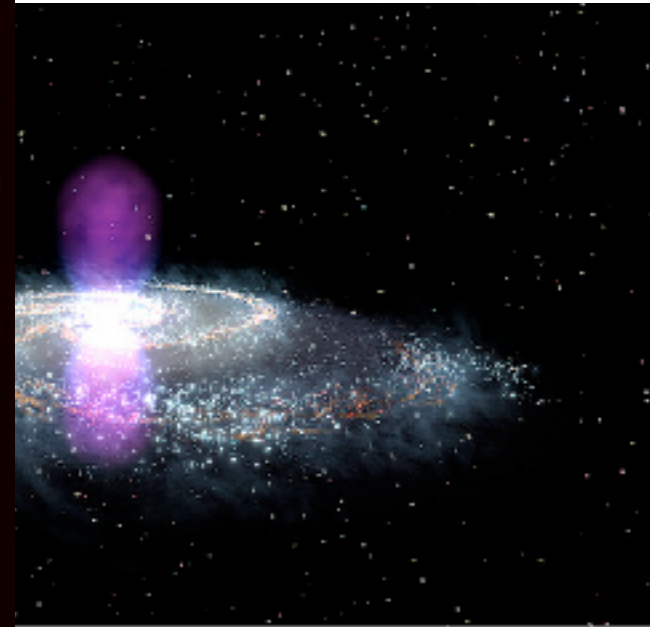
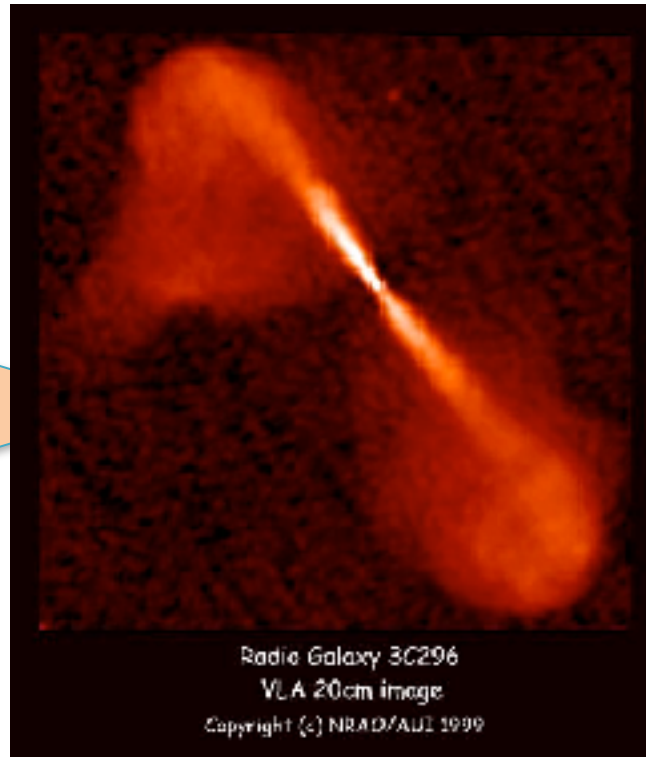
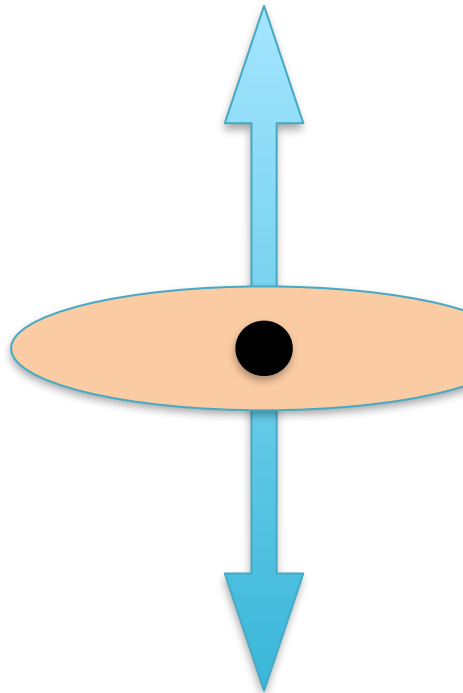
Geometry

- Height: 55° ; width: 45°
- centered at zero Galactic longitude
- symmetric about the Galactic plane
- Sharp edges
- Flat surface brightness: The surface brightness shows little variation over the bubbles

- The spectrum is uniform in different parts of the bubbles
- The spectrum is identical in both bubbles
- Harder spectrum, than the diffuse gamma-ray glow throughout the sky

The AGN Jet Model of the Fermi Bubbles

Bipolar Jets

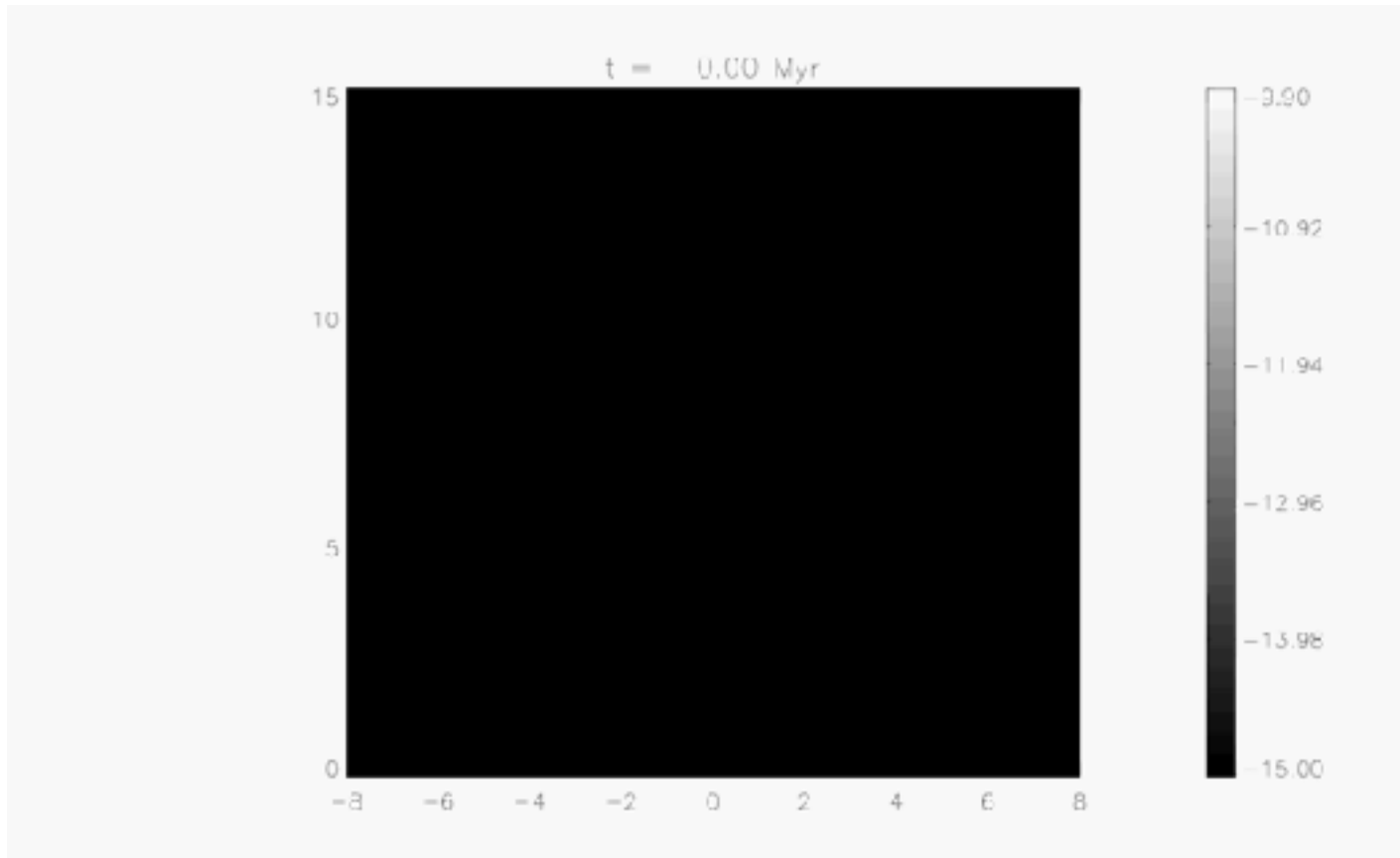


Fermi Bubbles

- Guo & Mathews 2012; Guo + 2012, ApJ

The Fermi Bubbles in the Milky Way

produced by a light internally-supersonic jet!



Guo & Mathews,
2012, ApJ

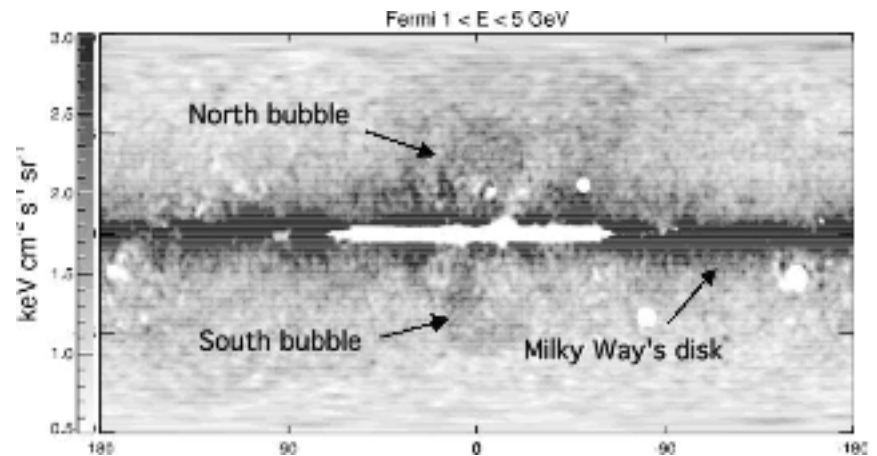
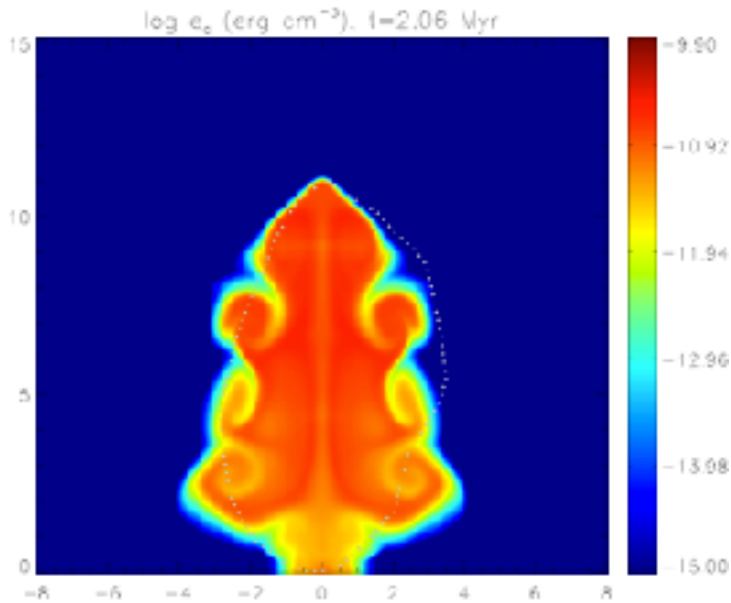
Guo et al, 2012, ApJ

cosmic ray distribution

Were the bubbles really produced by a recent jet event?

A recent jet event reproduces many bubble features: location, size, shape, sharp edges

CR particle distribution

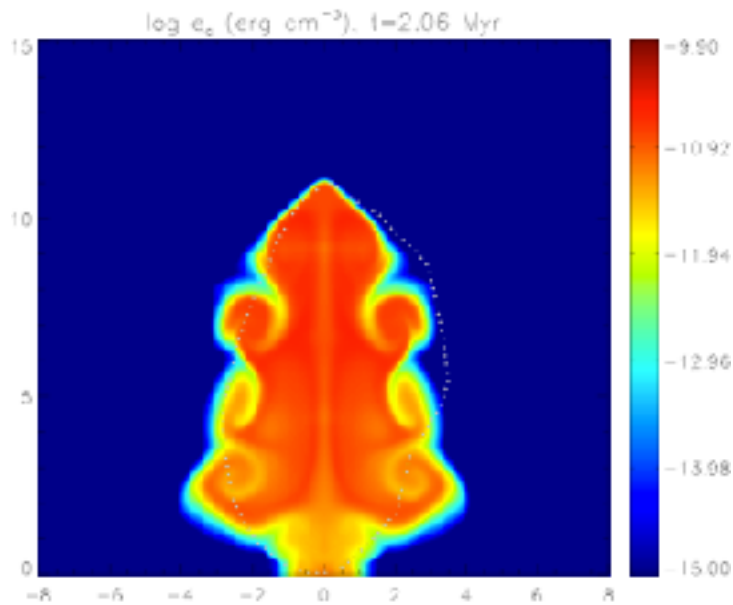


Guo & Mathews 2012

Su, Slatyer, and Finkbeiner, 2010

What are the energetics and age of the bubble event?

CR particle distribution

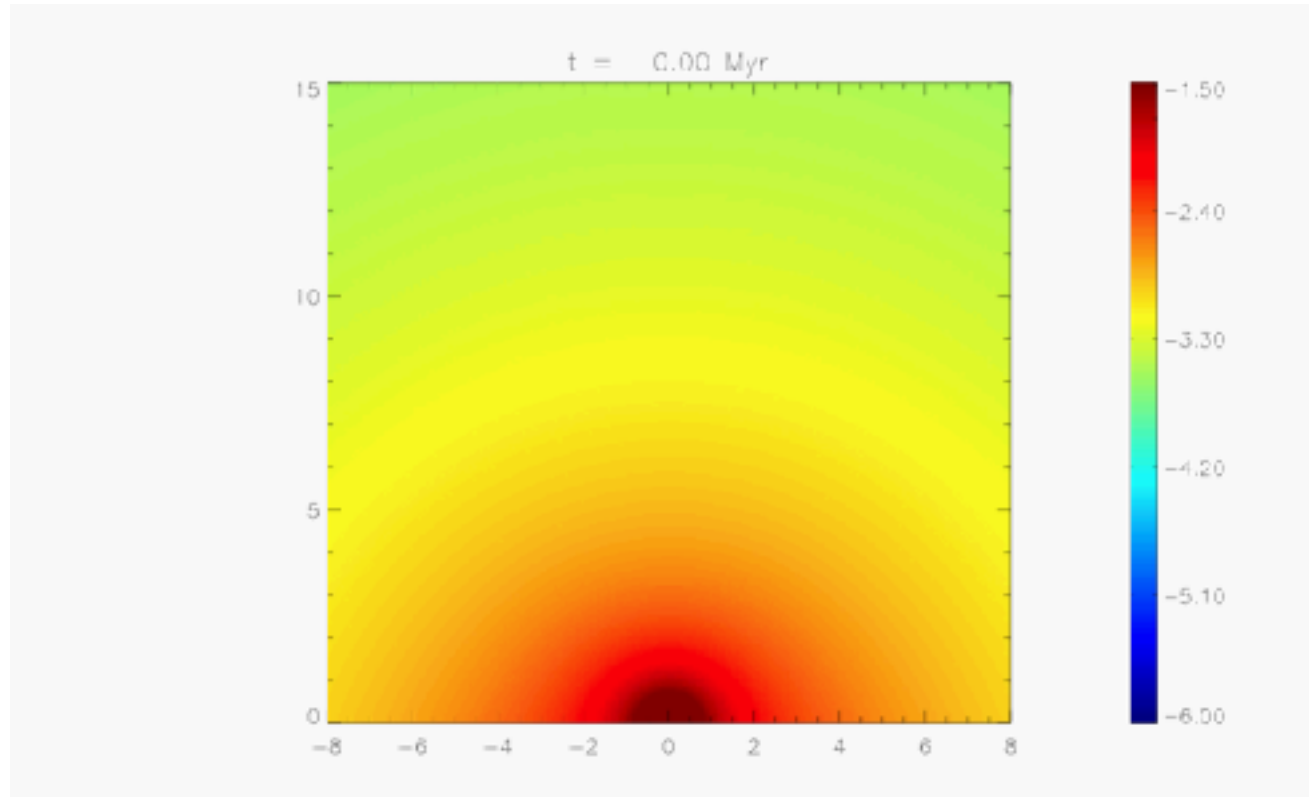


Guo & Mathews 2012

- (1) Energetics $\sim 10^{55} - 10^{57}$ erg
Age $\sim 1 - 3$ Myr
Jet duration $\sim 0.1 - 0.5$ Myr
Total mass that SMBH accreted:
 $\sim 100 - 10000 M_{\text{sun}}$

Impact on the Milky Way's gaseous halo

thermal gas density distribution

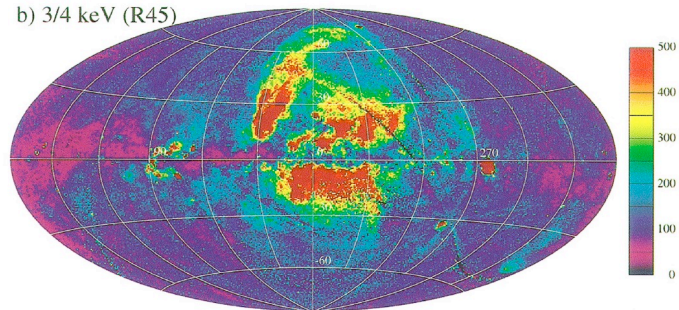


Guo & Mathews,
2012, ApJ

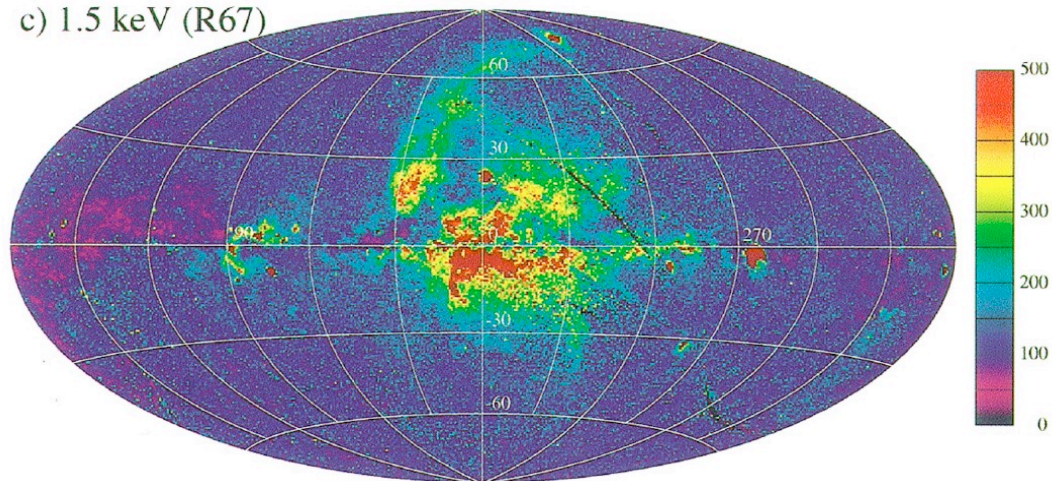
produce a forward shock and expansion of the inner gaseous halo

North Polar Spur in the ROSAT X-ray map

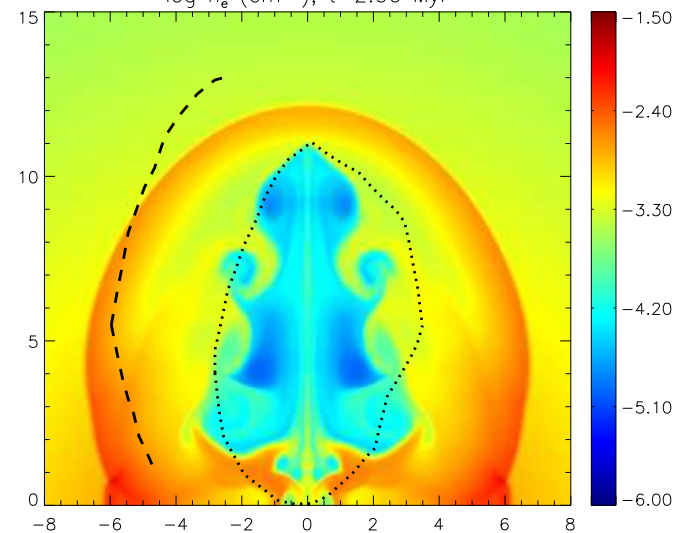
b) 3/4 keV (R45)



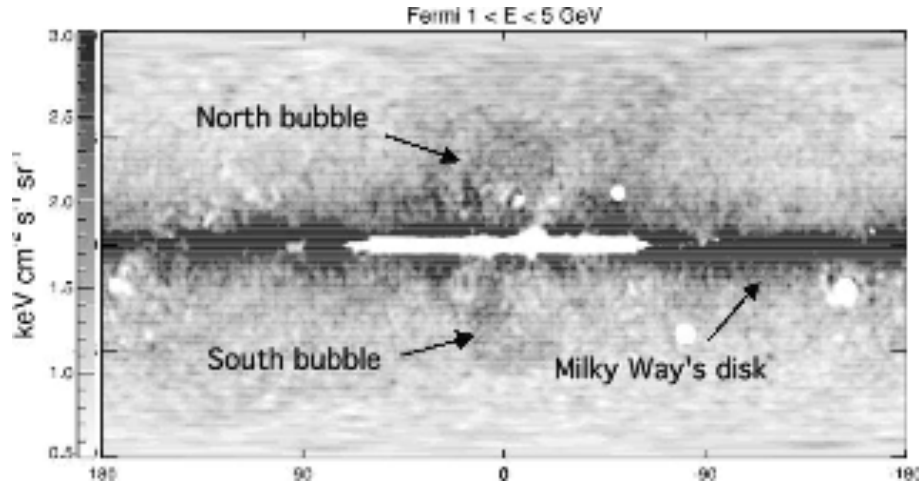
c) 1.5 keV (R67)



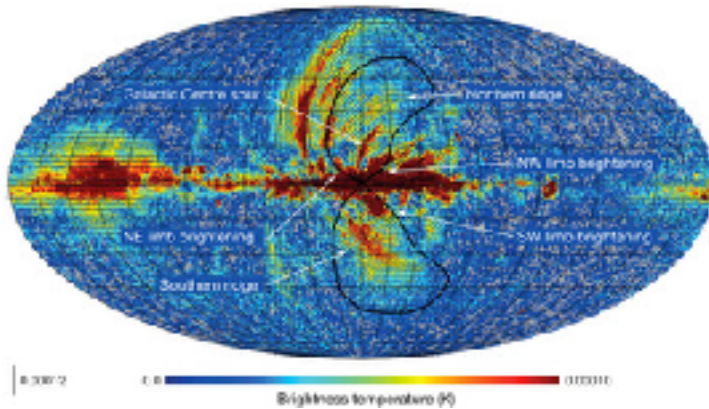
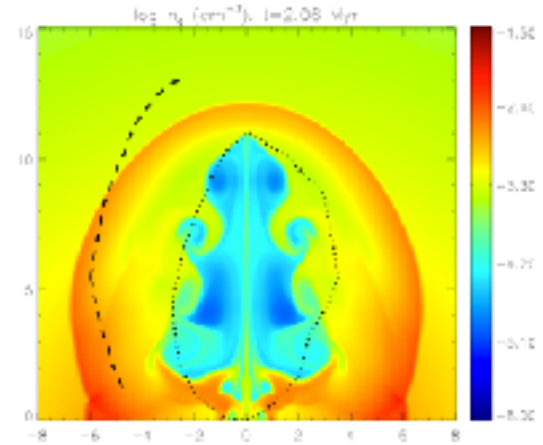
$\log n_e$ (cm^{-3}), $t=2.06$ Myr



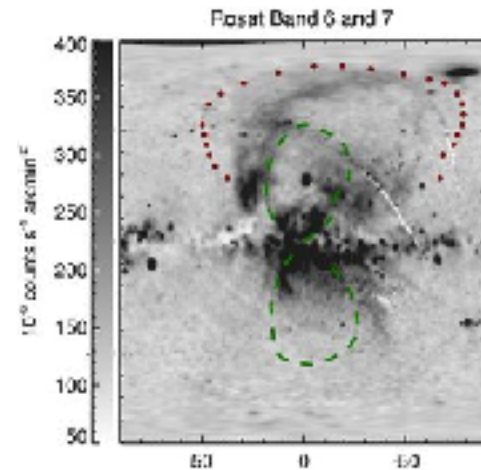
North Polar Spur



Gamma-ray North arc



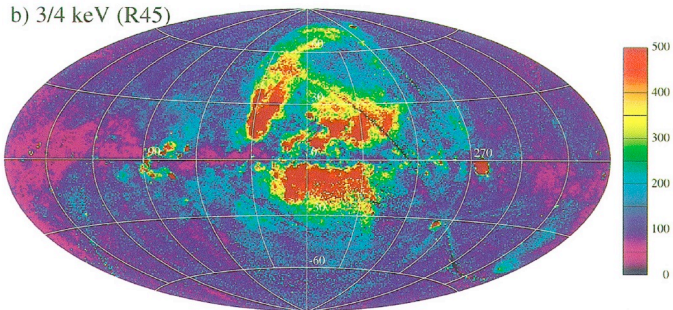
Polarized 23GHz emission by WMAP



ROSAT X-ray map and the bubbles₄₅

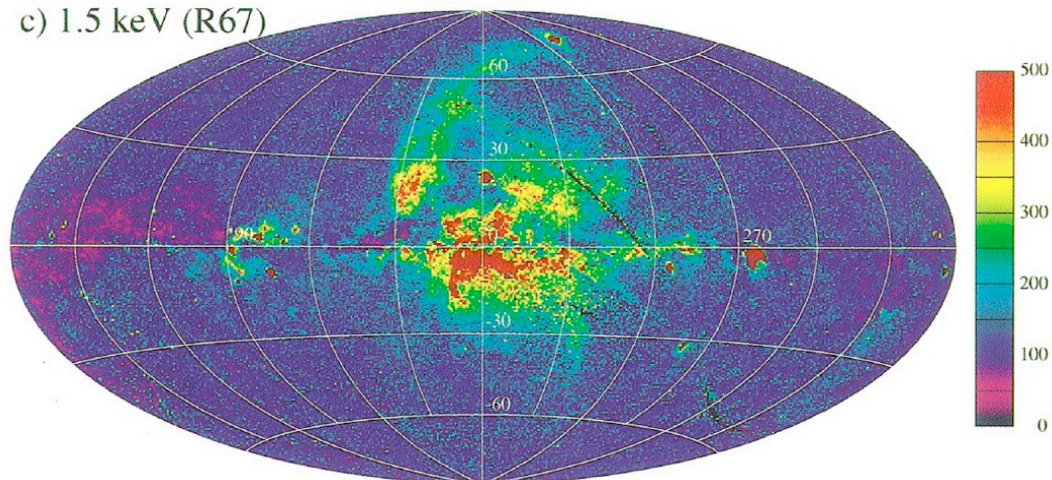
Where is the forward shock?

b) 3/4 keV (R45)

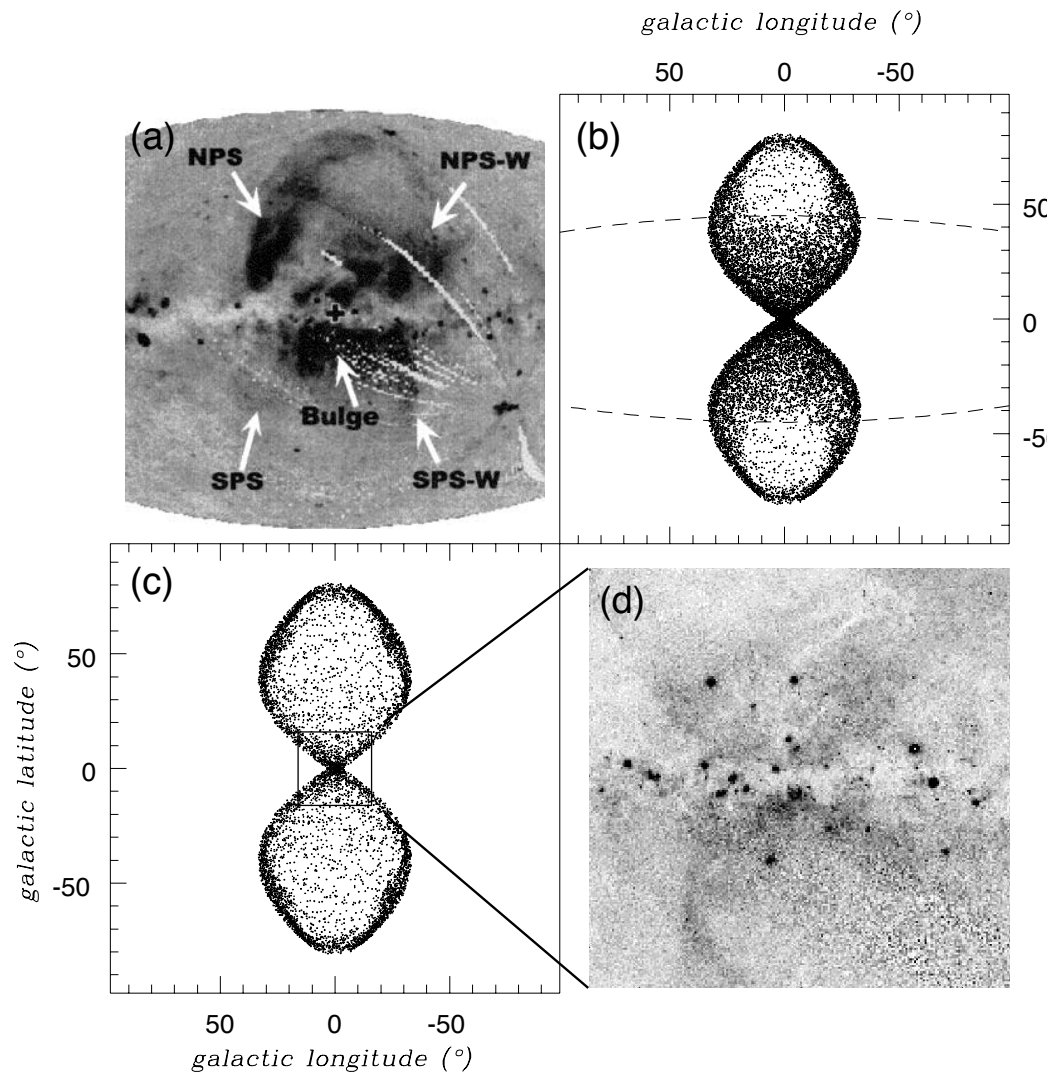


Joss Bland-Hawthorn

c) 1.5 keV (R67)

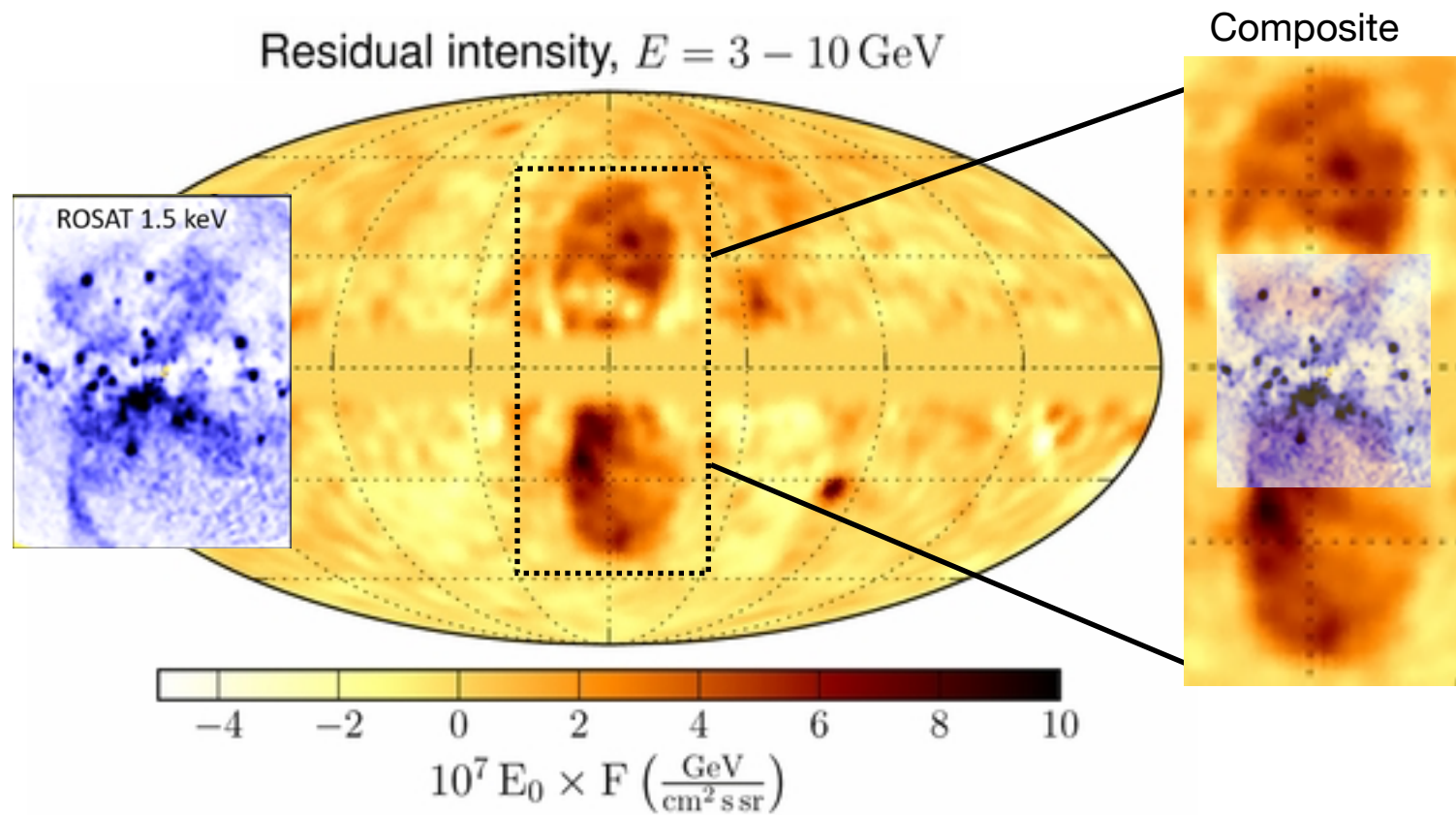


Where is the forward shock?



Bland-Hawthorn, J et al 2003

Where is the forward shock?



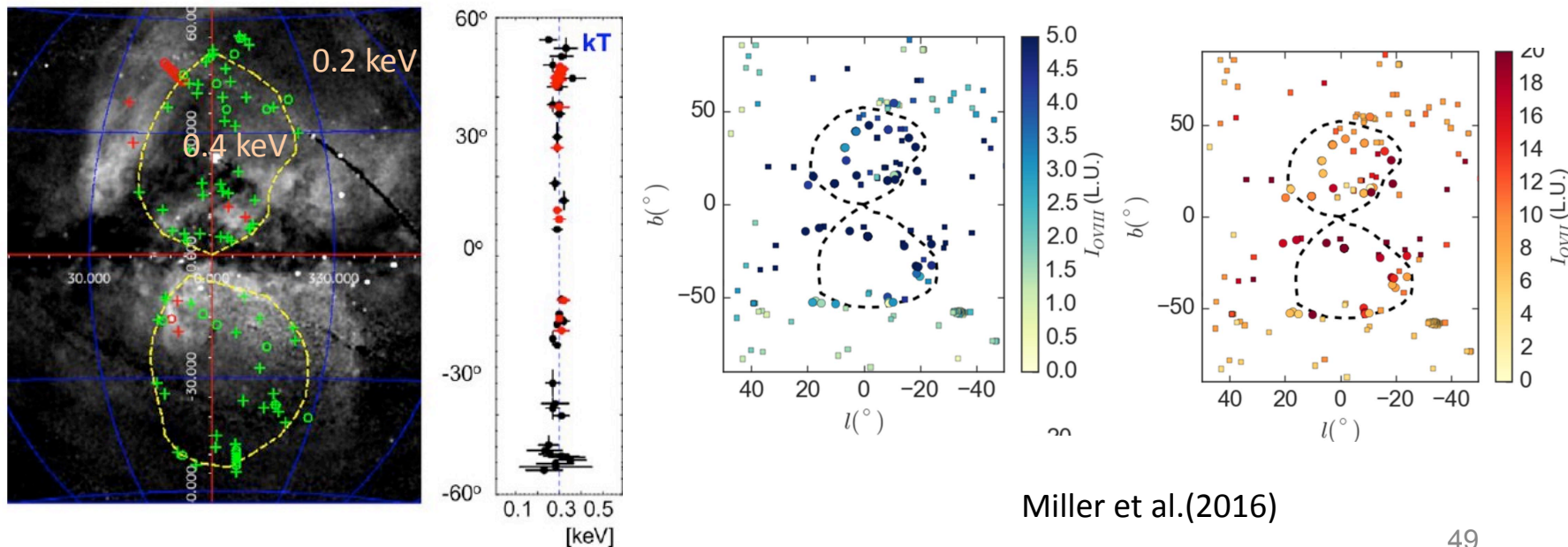
Observational Constraints on the Fermi Bubbles

Kataoka et al.(2015) found the bubble temperature is $kT \sim 0.30$ keV

Miller et al.(2016) found the bubble temperature is $kT \sim 0.40$ keV

Bordoloi et al.(2017) found the bubble age is 6-9 Myr from UV absorption line studies of HVCs towards the bubbles.

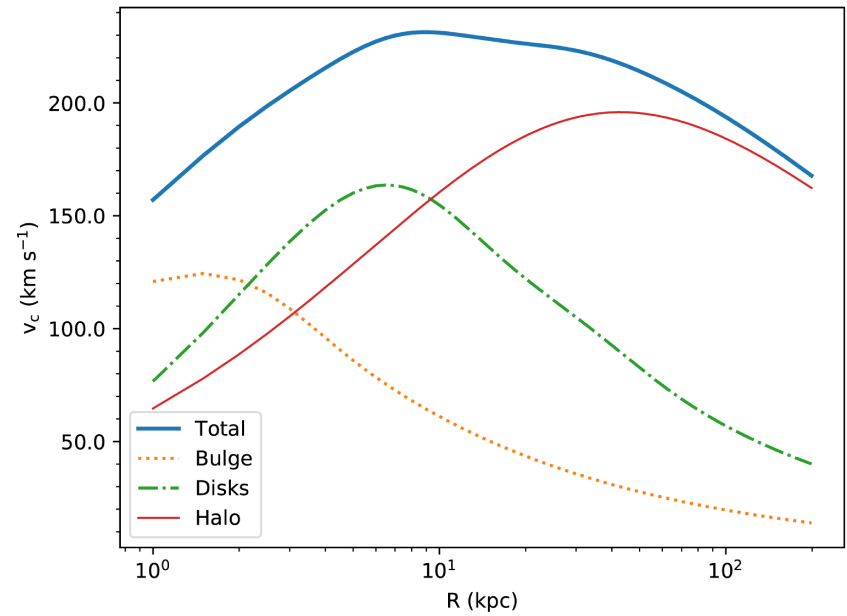
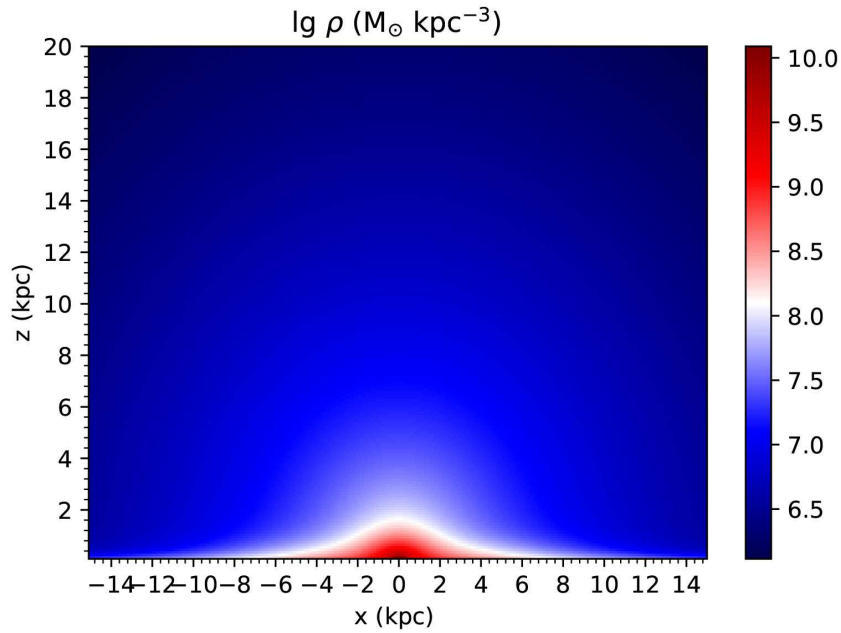
Sgr A* is orbited by over a hundred massive stars with ages $\sim 6 \pm 2$ Myr



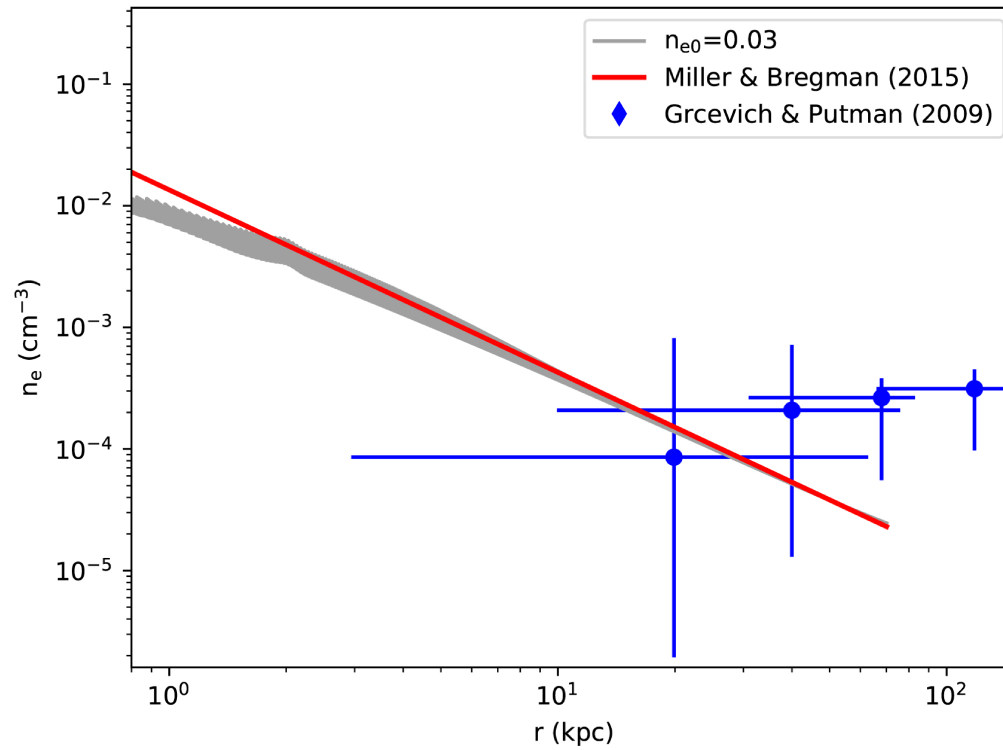


Ruiyu Zhang

The Total Matter Distribution in the Milky Way

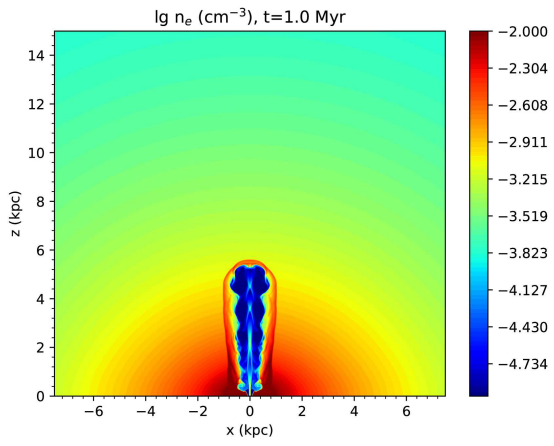


The CGM Distribution in the Milky Way

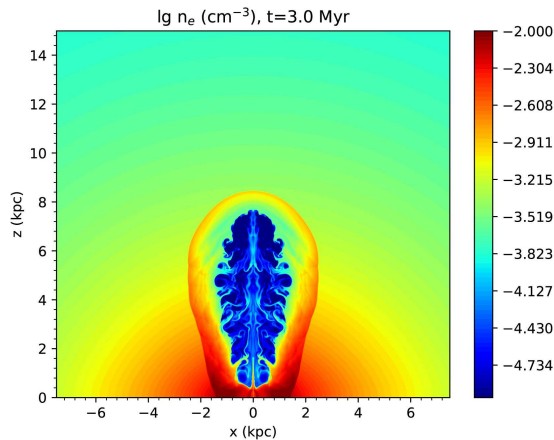


The Evolution of Fermi bubbles

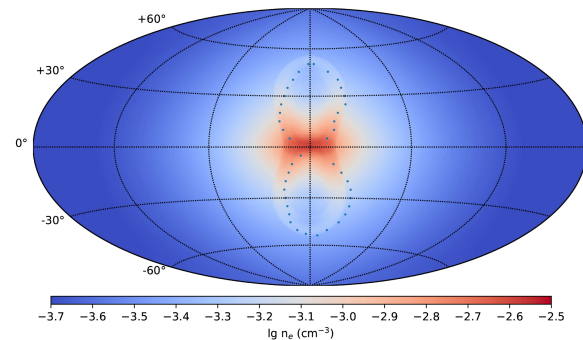
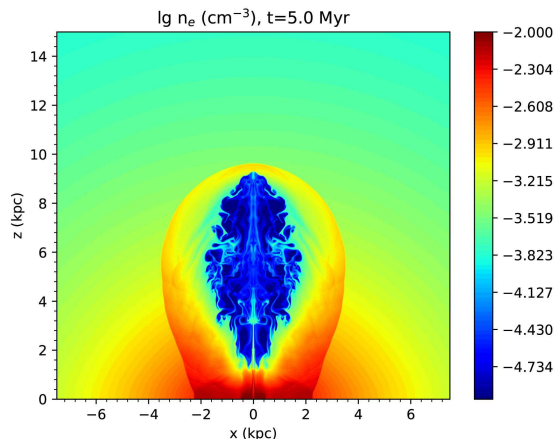
The energetics and age of the bubbles are constrained quite well!



(a)

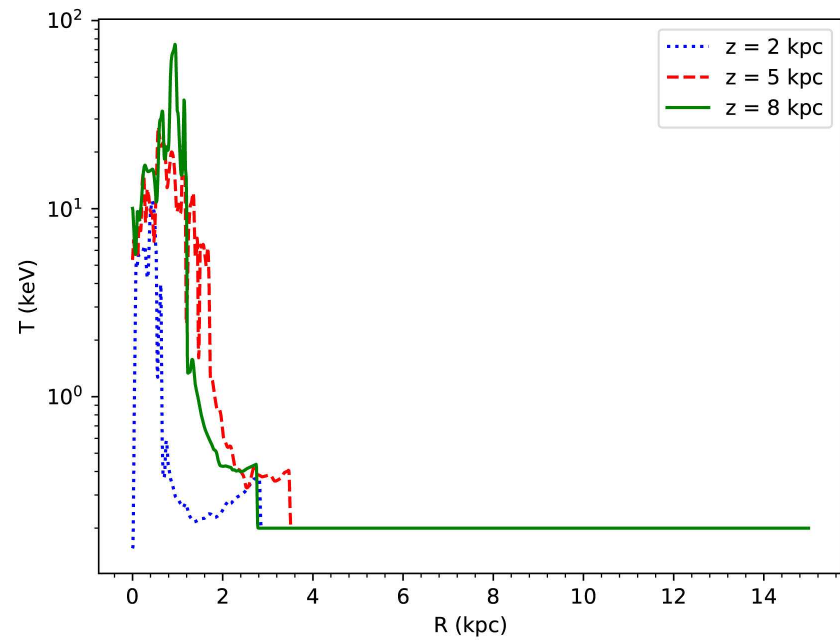
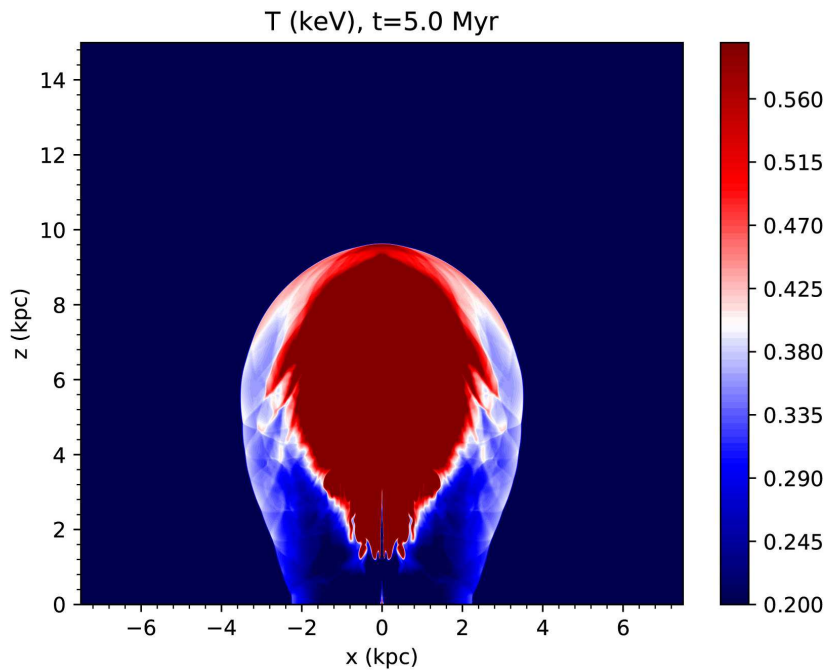


(b)



Projected Average Density

Gas temperature distribution



1.5 keV X-ray Surface Brightness Map

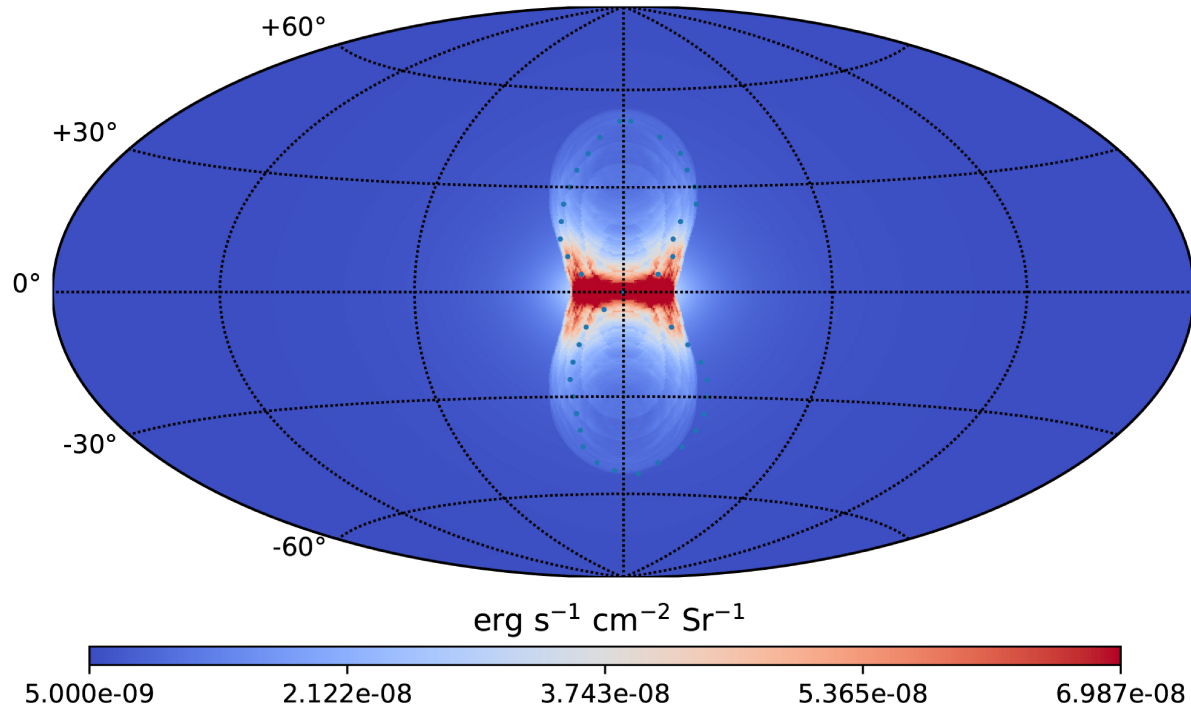


Figure 9. Synthetic X-ray (0.7–2 keV) surface brightness map in Galactic coordinates with a Hammer-Aitoff projection for run A at $t = 5$ Myr. The dots represent the edge of the observed Fermi bubbles.

Numbers for the Fermi bubbles

one Jet Power: $3.42 \times 10^{41} \text{ erg s}^{-1}$

Jet duration: 1 Myr

Current Fermi bubble age: 5 Myr

Total injected energy $\sim 2 \times 10^{55} \text{ erg}$

Eddington ratio: ~ 0.001 , hot accretion mode

Sgr A* accretion rate $\sim 0.0001 \text{ solar mass/yr}$

Wind Model

We performed a large number of wind simulations with different wind parameters (e.g. the wind velocity, density, and duration) and investigated if the spherical wind model can produce a bubble enclosed by the forward shock that meets both the temperature and morphology constraints as described in Section 3. Here we

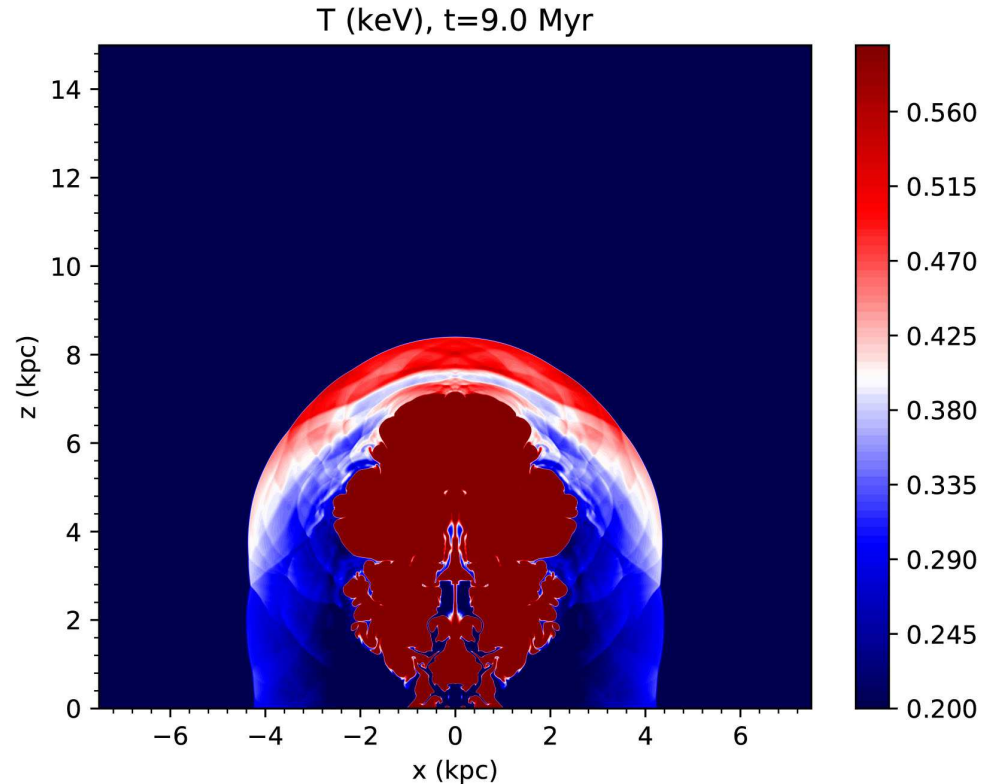


Figure 15. The temperature distribution of thermal gas at $t = 9$ Myr in run D for the spherical wind model.

The forward shocks driven by spherical winds at the GC typically produce bubbles with much wider bases than observed, and could not reproduce the biconical X-ray structure at low latitudes. This suggests that starburst or AGN winds are unlikely the origin of the bubbles in the shock scenario.

Particle Acceleration at the Shock Front

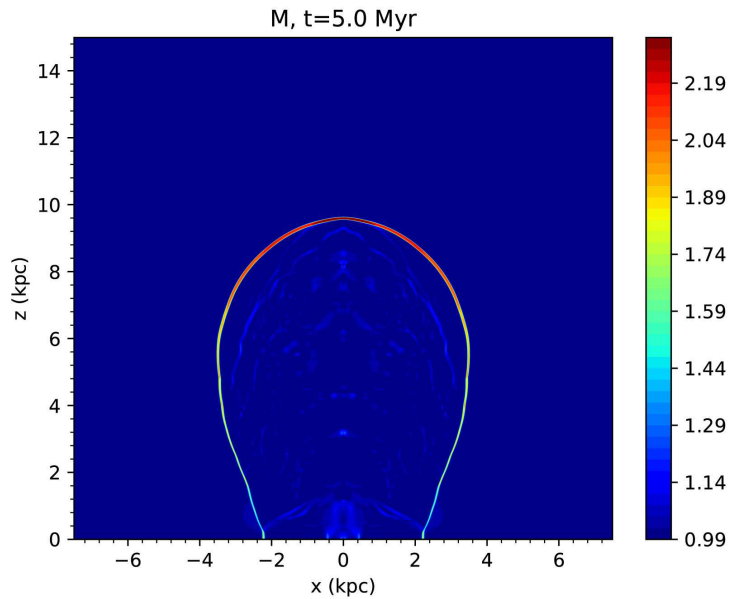


Figure 11. Mach number of the forward shock in Run A at $t = 5$ Myr. The Mach number increases from low to high latitudes, with an approximate value of about $M \sim 2$.

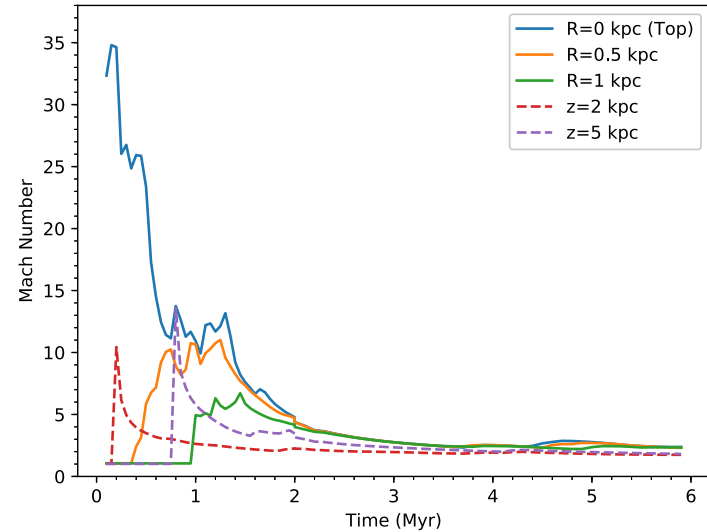


Figure 12. Temporal evolution of the Mach number of the forward shock in Run A. From top to bottom, the solid lines refer to the Mach number evolution at $R = 0$ (the bubble top), 0.5 kpc, and 1 kpc respectively, in the bubble surface. The dashed lines refer to the Mach number evolution at $z = 2$ kpc (red), and 5 kpc (purple) in the bubble surface.

Cooling and Heating Rates

Cooling rate of CGM (0.3 solar metallicity):

$$9.46 \times 10^{40} \text{ erg/s when } M_g = 0.3M_{\text{mbar}}$$

$$2.63 \times 10^{41} \text{ erg/s when } M_g = 0.5M_{\text{mbar}}$$

$$1.06 \times 10^{42} \text{ erg/s when } M_g = M_{\text{mbar}}$$

Supernova heating rate: $6.03 \times 10^{41} \text{ erg/s}$
(1.9 SN per century)

AGN feedback heating rate: $1.27 \times 10^{40} \text{ erg/s}$.
(One Fermi bubble event per 50 Myr)

Outstanding Problems

- Does the shock model produce cosmic rays radiating the observed gamma rays?
- How are cosmic rays accelerated in the Fermi bubbles?
- What about the origin of the North Polar Spur?
- Are Fermi bubbles common in disk galaxies?
- How does Fermi-bubble-like events affect the CGM of Milky Way like galaxies?
- Does AGN feedback transform star forming Milky-Way-like galaxies into quenched S0 galaxies? If so, when does this happen for a typical disk galaxy?

Summary

- We propose a physically motivated model for the Milky Way CGM
- We propose a new method to measure the Milky Way mass based on the CGM temperature, $M_{\text{vir}} = 1.60_{-0.41}^{+1.35} \times 10^{12} M_{\odot}$
- Without heating sources, cooling flows are expected to develop in the Milky Way CGM, leading to typical mass inflow rates of 5-10 solar mass per year, about 5 times larger than the star formation rate. Stellar feedback may be more important than AGN feedback in heating the CGM.
- We propose a forward-shock model for the Fermi bubbles, which were formed by a pair of jets emanating from Sgr A* about 5 Myr ago. This model explains the common origin of the Fermi bubbles and the Galactic center X-ray outflows. The energy and age of the bubbles are well constrained in this model.
- Wind models could not explain the Fermi bubbles in the shock scenario.